

**CO₂ ENRICHMENT IN AMBIENT AIR BY TEMPERATURE SWING
ADSORPTION AND ITS APPLICATIONS FOR STIMULATING PLANT
GROWTH IN GREENHOUSES**

by

Jie Bao

B.A.Sc, China University of Petroleum (Beijing), 2011

A THESIS SUBMITTED IN PARTIAL FULFILLMENT OF THE REQUIREMENTS FOR THE
DEGREE OF

MASTER OF APPLIED SCIENCE

in

THE FACULTY OF GRADUATE AND POSTDOCTORAL STUDIES

(Chemical and Biological Engineering)

THE UNIVERSITY OF BRITISH COLUMBIA

(Vancouver)

April 2014

© Jie Bao, 2014

Abstract

Adsorption on proper adsorbents is one of the commonly used technologies to capture carbon dioxide. Zeolites, such as 13X, exhibit good adsorption capacity and selectivity towards CO₂. Compared with CO₂ capture from large point sources with high concentration of CO₂, direct capture from the ambient air plays a better role in the reduction of greenhouse gases. On the other hand, greenhouse crops can be benefited from CO₂ enrichment, typically around 1000 ppm. By applying temperature swing adsorption (TSA) to ambient air, CO₂ concentration can be enriched from 400 ppm to about 1000 ppm, which can then be directly used for greenhouse CO₂ enrichment. The proposed method not only helps the capture of CO₂ from air but also provides an enriched CO₂ stream to greenhouses.

In this study, the performance of zeolite 13X was evaluated in a fixed bed reactor for enriching ambient CO₂ concentration from 400 ppm to 1000 ppm by temperature swing adsorption under different operating conditions such as ambient temperature and moisture content. Results showed that 13X performed well for both CO₂ adsorption and desorption, and an enrichment factor of 3 can be reached, demonstrating the feasibility of the proposed TSA method. A lower adsorption temperature and a higher desorption temperature would result in a higher enriched CO₂ concentration.

Finally, economic analyses have been carried out to compare the unit cost of proposed method for capturing one tonne CO₂ with the cost of other air capture technologies and the cost of CO₂ supply in current greenhouse operations. The unit cost of CO₂ enrichment by temperature swing adsorption seems to be quite competitive if the adsorption and desorption capacity of the currently tested adsorbent could be increased by six times to the level as reported in the literature.

Preface

This thesis is original, unpublished and independent work of the author, Jie Bao, under the supervision of Dr. Xiaotao Bi.

Table of contents

Abstract.....	ii
Preface.....	iii
Table of contents	iv
List of tables.....	viii
List of figures	ix
Abbreviation	xii
Acknowledgements.....	xv
Chapter 1 Introduction	1
1.1 Greenhouse gas emissions and control.....	1
1.2 CO ₂ enrichment in greenhouses	3
1.3 CO ₂ capture from ambient air for greenhouse uses.....	4
1.4 Research objectives	5
1.5 Organization of the thesis.....	6
Chapter 2 Literature review	7
2.1 Capturing CO ₂ directly from ambient air	8
2.1.1 CO ₂ capture from air by absorption and adsorption	10

2.1.2 Different methods for CO ₂ capture from air by adsorption	15
2.2 13X zeolite for CO ₂ adsorption	17
Chapter 3 Experimental setup and procedures.....	24
3.1 Materials and methods.....	24
3.1.1 Materials	24
3.1.2 Methods.....	24
3.2 Experimental setup and procedures.....	25
Chapter 4 Experimental results and discussions.....	30
4.1 Influence of desorption flow rate	30
4.1.1 Purpose.....	30
4.1.2 Experimental conditions	30
4.1.3 Results and discussions.....	31
4.2 Experiments with 1000 ppm CO ₂	34
4.2.1 Experimental conditions	34
4.2.2 Results and discussions.....	35
4.3 Experiments with 400 ppm CO ₂	41
4.3.1 Experimental conditions	41
4.3.2 Results and discussions.....	42

4.3.3 Experimental error analyses.....	46
4.3.4 Correlations for adsorption capacity.....	50
4.4 Moisture effects.....	51
4.4.1 Experimental setup.....	51
4.4.2 Results and discussions.....	53
4.5 Summary	56
Chapter 5 Economics analyses.....	57
5.1 Cost analyses of CO ₂ enrichment by TSA directly from air	57
5.1.1 Capital cost.....	57
5.1.2 Operating cost	58
5.1.3 Unit price of CO ₂	59
5.1.4 Sensitivity analysis of CO ₂ unit price to the adsorbent performance	63
5.2 Costs for different scenarios to provide heat and CO ₂ to greenhouses	66
5.3 Costs for using other methods to capture CO ₂ directly from air	68
5.4 Comparison of costs for CO ₂ -enrichment for greenhouses.....	69
5.5 Summary	70
Chapter 6 Conclusions and future work.....	71
6.1 Conclusions	71

6.2 Future work	72
References	73

List of tables

Table 4-1 Adsorption capacity, desorption capacity and peak concentration (1000 ppm CO ₂)....	35
Table 4-2 Adsorption capacity, desorption capacity and peak concentration (400 ppm CO ₂).....	42
Table 4-3 Error analyses for several repeated experiments with 400 ppm CO ₂	47
Table 4-4 Peak moving average concentrations with a RH of 20% at different temperatures	56
Table 5-1 Capital costs at different adsorbent loadings	61
Table 5-2 Main assumptions used in the calculation	62
Table 5-3 Sensitivity analyses of CO ₂ unit price to desorption capacity	65
Table 5-4 Different scenarios to provide heat and CO ₂ to greenhouses	67
Table 5-5 Cost of CO ₂ capture by different air capture technologies	69

List of figures

Figure 1-1 Scenarios of Canadian emissions to 2020 (Mt CO ₂ e) ²	2
Figure 1-2 Illustration of CCS and CO ₂ enrichment and application	5
Figure 2-1 Three steps in CCS.....	7
Figure 2-2 Global greenhouse gas emissions by sources.....	9
Figure 2-3 Sodium hydroxide air capture system.....	11
Figure 2-4 Diagram of prototype contactor	12
Figure 2-5 Moisture swing adsorption of CO ₂ on a quaternary ammonium functionalized ion exchange membrane.....	14
Figure 2-6 Classification of supported amine adsorbents.....	16
Figure 2-7 Adsorption isotherm of CO ₂ on different sorbents at 295 K.....	18
Figure 2-8 Adsorption isotherms of CO ₂ on various adsorbents	20
Figure 2-9 Carbon dioxide adsorption isotherms on various adsorbents	21
Figure 2-10 CO ₂ adsorption isotherms at 333K	22
Figure 3-1 Model 906 CO ₂ analyzer.....	25
Figure 3-2 Process diagram of CO ₂ adsorption and desorption unit	26

Figure 3-3 CO ₂ adsorption and desorption unit	27
Figure 3-4 Adsorption of CO ₂ from 1000 ppm CO ₂ and balanced N ₂ gas mixture at 10 °C and desorption at 30 °C	28
Figure 4-1 Moving average concentrations with an adsorbent loading of 5 g.....	31
Figure 4-2 Moving average concentrations with an adsorbent loading of 10 g.....	32
Figure 4-3 Moving average concentrations with an adsorbent loading of 20 g.....	32
Figure 4-4 Peak moving average CO ₂ concentration as a function of desorption flow rate.....	34
Figure 4-5 Enrichment factor as a function of desorption time (1000 ppm CO ₂ , ΔT=20 °C)	36
Figure 4-6 Enrichment factor as a function of desorption time (1000 ppm CO ₂ , ΔT=15 °C)	37
Figure 4-7 Enrichment factor as a function of desorption time (1000 ppm CO ₂ , ΔT=10 °C)	37
Figure 4-8 Enrichment factor as a function of desorption time (1000 ppm CO ₂ , ΔT=5 °C)	38
Figure 4-9 Adsorption capacity versus adsorption temperature at four different adsorption-desorption temperature differences (1000 ppm CO ₂)	39
Figure 4-10 Desorption capacity as a function of desorption temperature (1000 ppm CO ₂)	40
Figure 4-11 Maximum enrichment factor at different adsorption temperatures (1000 ppm)	41
Figure 4-12 Enrichment factor as a function of desorption time (400 ppm CO ₂ , ΔT=20 °C)	43

Figure 4-13 Enrichment factor as a function of desorption time (400 ppm CO ₂ , ΔT=15 °C)	43
Figure 4-14 Enrichment factor as a function of desorption time (400 ppm CO ₂ , ΔT=10 °C)	44
Figure 4-15 Adsorption capacity versus adsorption temperature at four different adsorption-desorption temperature differences (400 ppm)	45
Figure 4-16 Desorption capacity as a function of desorption temperature (400 ppm)	45
Figure 4-17 Maximum enrichment factor at different adsorption temperatures (400 ppm)	46
Figure 4-18 Average adsorption capacity, desorption capacity and peak moving average concentration with error bars included	49
Figure 4-19 Data fitting to Freundlich model equation	50
Figure 4-20 Process diagram of CO ₂ adsorption and desorption unit with humidification setup	52
Figure 4-21 Humidifier setup.....	52
Figure 4-22 Adsorption capacities at different RH	53
Figure 4-23 Desorption capacities at different RH	55
Figure 5-1 Purchased equipment cost.....	60
Figure 5-2 CO ₂ unit price as a function of daily operation cycles at different adsorbent loadings	63
Figure 5-3 Sensitivity analyses of unit price to adsorbent price and adsorption capacity	66

Abbreviation

CCS	Carbon capture and storage
TSA	Temperature swing adsorption
PSA	Pressure swing adsorption
T_{ad}	Adsorption temperature
T_{de}	Desorption temperature
C_{in}	Inlet CO ₂ concentration
C_{out}	Outlet CO ₂ concentration
Q_{in}	Inlet gas flow rate
Q_{out}	Outlet gas flow rate
q_{ad}	Adsorption capacity
q_{de}	Desorption capacity
t_{ad}	Adsorption time
t_{de}	Desorption time
f	Enrichment factor
$c(ave)$	Moving average CO ₂ concentration in the outlet gas stream
$c(ave)_{max}$	Peak moving average CO ₂ concentration in the outlet gas stream

ΔT	Temperature difference between adsorption and desorption temperature
k	Parameter in Freundlich model equation
n	Parameter in Freundlich model equation
C_{cap}	Annualized capital cost
PV	Present value
m	Lifetime of the unit
i	Effective annual interest rate
Q	Gas flow rate in the industrial unit
Q_{exp}	Gas flow rate in the laboratory unit
M	Adsorbent loading in the industrial unit
M_{exp}	Adsorbent loading in the laboratory unit
a	Specific surface area
u	Superficial velocity
d_p	Average particle diameter
ΔP	Pressure drop across the bed
L	Length of the bed
D	Diameter of the bed

ε	Void fraction of the bed
μ	Viscosity of the air
ρ	Density of the air
E_{elec}	Electricity consumption
C_{elec}	Cost of electricity
η	Energy efficiency of air blower
p	Number of daily adsorption and desorption cycles

Acknowledgements

I would like to express my sincerest appreciation to my supervisor Dr. Xiaotao Bi, who gave me the opportunity to study at such a fabulous place. I'm truly thankful for his endless kindness, continuous support, and patient guidance to both my personal and academic development. His insightful suggestions and detailed instructions to my research have helped me with the successful completion of MASc program. I cannot think of a better supervisor to have, and I feel extremely proud and honored to be mentored by such a brilliant professor.

My deep gratitude is also extended to the committee members Dr. Jim Lim and Dr. Anthony Lau for attending my examination, for taking the time to read my thesis and for their valuable advices.

I'm grateful to all the CHBE faculty, staff and students for creating a friendly environment. I appreciate the hard work of administrative staff for their enormous administrative assistance. Great thanks are given to Richard Ryoo for his fast and effective responses to my ordering requests. Also I'd like to thank CHBE workshop for helping me with the setting up of my unit. Special thanks are given to Dr. Zhiwei Chen for always answering my questions patiently while conducting experiments.

I would like to greatly acknowledge Xingxing Cheng, Di Li, Mingming Yu and Xu Zhao for their continuous support and unforgettable friendship during these two years. I wish to thank my friends in China for their concerns despite of the far away distance. I'd like to offer gratitude to all friends in Vancouver who make my life meaningful and memorable in this beautiful place.

Last but not least, great gratitude is owed to my parents for their endless love and continuous encouragement throughout my life.

Chapter 1 Introduction

1.1 Greenhouse gas emissions and control

The world is enjoying a boom in economics and new technologies, resulting in the environmental problems as well, such as global warming, acid rain formation, smog formation, etc. Among all these problems, global warming, resulting from the emission of greenhouse gases mainly carbon dioxide, is considered as the most serious one.

Carbon dioxide (CO₂) can be produced from various sources, such as fossil fuel combustions, biomass energy facilities, large power plants in industrial processes, etc. Due to the increasing consumption of fossil fuels by humans as needed in the industry, CO₂ concentration in the atmosphere has increased from 270 ppm in pre-industrial period to nearly 400 ppm at present[1]. The increasing concentration of carbon dioxide, a major composition of greenhouse gases, has brought about serious environmental problems, including ice melting, sea level rising, and ocean acidification[2]. The global average temperature has been increased by 0.8 °C over the past century as a result of the accelerating global warming[3]. The earth is suffering from the ever increasing burning of carbon, and the irreversible damage to the earth's ecosystems would be so extensive that civilized human beings have never experienced [4]. The increase of carbon dioxide in the atmosphere has given rise to so many issues that couldn't be ignored and require critical attentions and immediate solutions. As a result, carbon management was proposed as a means of reducing global carbon dioxide emissions in the world to mitigate this problem.

As an Arctic nation, the climate change in northern area will definitely have a great impact on Canada. It is everyone's responsibility to engage in reducing greenhouse gas emissions. As a signatory to the United Nations Framework Convention on Climate Change (UNFCCC), Canada has always been seeking opportunities to reduce greenhouse gas emissions by exploring carbon

capture and storage. After failed to achieve its Kyoto Protocol target, Canada signed onto the Copenhagen Accord in December 2009 and committed to reduce its greenhouse gas emissions to 17% below 2005 levels by 2020[5]. According to the latest National Inventory Report (NIR), Canadian GHG emissions decreased by 4.8%, between 2005 and 2011, while the economy grew by 8.4% over the same period[5]. Canada’s carbon dioxide emissions from fuel combustion in 2010 accounted for 1.8% of global emissions, down from 2.1% in 2005[5].

The analysis of Canada’s Emissions Trends (Figure 1-1) indicates that Canada’s GHG emissions would increase up to 862 Mt/year in 2020 if no government measures are taken. However, even considering all current measures and controls from citizens and governments, the emissions can only be controlled to 734 Mt/year in 2020, which is still far from the targeted 612 Mt/year.

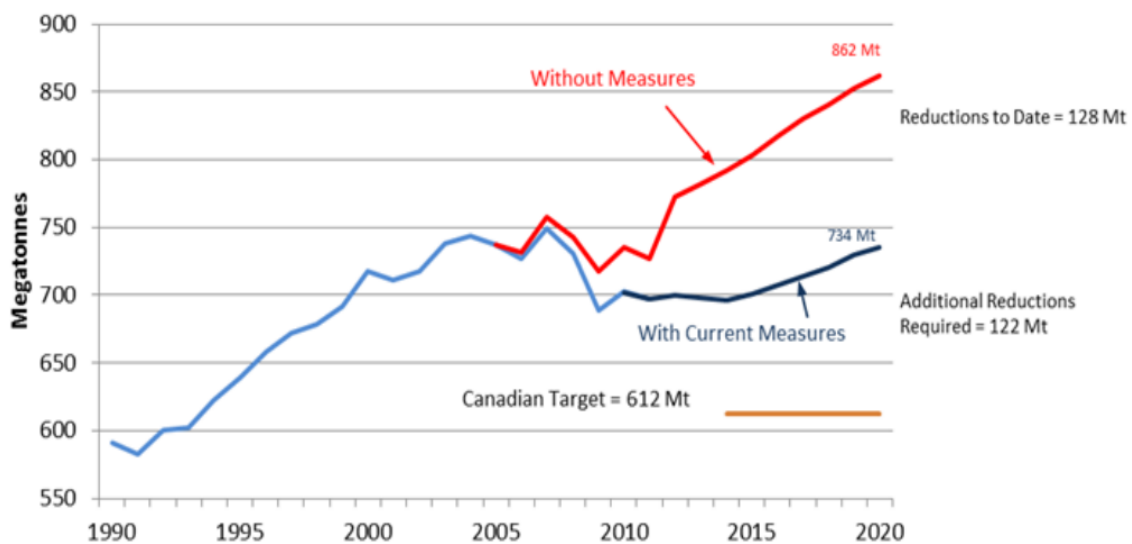


Figure 1-1 Scenarios of Canadian emissions to 2020 (Mt CO₂e)²

Researchers have proposed a plan, which is called carbon capture and sequestration (CCS), to deal with this problem. To remove CO₂ from gas mixtures, there are several possible approaches, including membrane separation, cryogenic distillation, chemical absorption and physical adsorption[6]. Up to now, most of the work has been done on the CO₂ capture from gas mixtures

which contain high concentrations of CO₂, such as flue gases from thermal power plants. Actually, nearly one third ^[3] of the carbon emissions are released from distributed sources like transportation vehicles, which are hard to be captured. Consequently, there's a demand to develop "on-site" carbon sequestration technologies. One possible approach is to capture CO₂ directly from the ambient air. By doing so, CO₂ emissions from all sources are dealt with, regardless of the location of point sources. This idea was first suggested by Lackner et al. (1999) as a method to address the global warming problem[7, 8]. The preliminary analysis on cost and energy required showed its feasibility for carbon removal from the atmospheric air.

In a typical CCS process, CO₂ is captured, transported and finally stored in a secure and safe storage site. However, despite of the costly capturing process, transportation and safe storage also account for parts of the total cost. To make full use of the captured CO₂ instead of just putting it into safe storage motivated us to explore the use of carbon dioxide to stimulate plant growth in greenhouses.

1.2 CO₂ enrichment in greenhouses

From the agriculture point of view, growth of crops is closely related to the concentration of CO₂ in the atmosphere they are exposed to. Carbon dioxide is fixed and converted into sugars during photosynthesis, which plays a significant role in plant growth. Most of the common greenhouse crops are less efficient in fixing CO₂ at ambient CO₂ levels[9]. Therefore enrichment of CO₂ in greenhouses is essential. It has been reported that commercial greenhouse crops, such as fruits, flowers and vegetables [10-12], benefit greatly from CO₂ enrichment, including increased yield, improved productivity and reduced demand in sunlight irradiance[9]. Typically, an increase of CO₂ concentration from 400 ppm to 1000 ppm will lead to a yield increase by 21% to 61% [10, 12-17]. On the other hand, the high CO₂ concentration also promotes of hormonal responses in terms of enhanced secondary compounds such as essential oils and antioxidants [18, 19].

Nowadays, CO₂ enrichment is commonly practiced as an effective way to enhance photosynthesis of crops in greenhouses. Carbon dioxide in greenhouses is usually obtained by burning carbon-based fuels such as natural gas, propane, and kerosene, or directly from tanks of pure CO₂. Each source has its own advantages and drawbacks. Liquefied CO₂ from pressurized tanks is a common option, which is safe and easy to be facilitated [12], although it is the most expensive option. Burning fuels can provide not only CO₂ but also heat to the greenhouse. The combustion needs to be carefully controlled to avoid plant damage by air pollutants such as NO_x and SO_x. On the other hand, the heat generated from the burning of fuels may be wasted in summer when heating is not required for greenhouses. If the captured CO₂ from air can be applied into greenhouses for plant use, it will provide an alternative for CO₂ capture and sequestration.

1.3 CO₂ capture from ambient air for greenhouse uses

Typically, the CO₂ concentration required for a greenhouse is about 1000 ppm, while CO₂ in the ambient atmosphere is 400 ppm. If the CO₂ concentration in the air can be enriched from 400 ppm to the target concentration of 1000 ppm at a cost much lower than pure CO₂ captured for secure storage, then it would be feasible to capture CO₂ from atmospheric air and then use it directly for greenhouses to stimulate the crop growth. There has been no analysis being carried out or reported in the literature, and this forms the basis for this study.

Other than the traditional CO₂ capture and storage route, we propose a new approach to not only capture CO₂ from the atmosphere, but also to provide an enriched CO₂ stream to greenhouses for plant growth stimulation. The differences between these two methods can be illustrated in Figure 1-2. The CO₂ sources are ambient air, instead of the widely used flue gases. More importantly, instead of capturing CO₂ to high concentrations for storage, the concentration would be enriched by temperature swing adsorption from 400 ppm to the desired level of 1000 ppm, which is expected to incur a lower operating cost. Furthermore, CO₂ will not be compressed, transported

and disposed to a secure storage site, which will reduce the relevant transportation and storage costs. As well, the enriched CO₂ stream can be directly applied in greenhouse, generating a saving from replaced CO₂ sources.

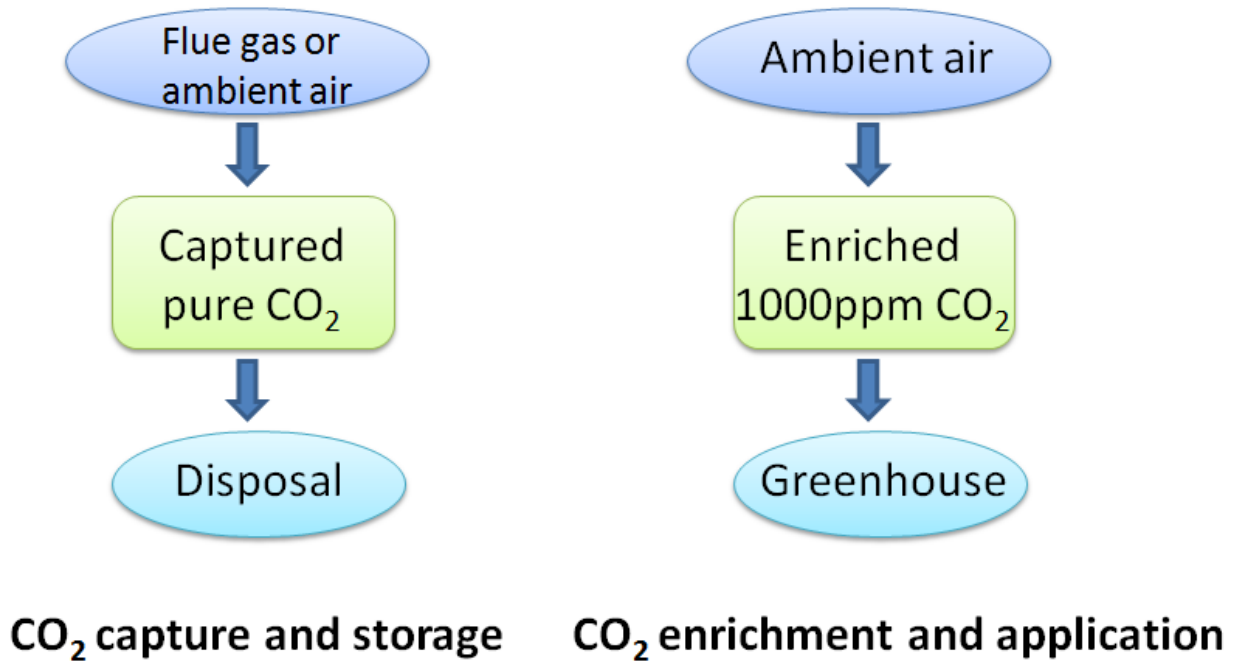


Figure 1-2 Illustration of CCS and CO₂ enrichment and application

1.4 Research objectives

The research objectives of this proposed study are:

- 1) To experimentally evaluate the performance of selected adsorbents for enriching ambient CO₂ concentration from 400 ppm to 1000 ppm by temperature swing adsorption.
- 2) To conduct an economic analysis on the proposed method and to compare the cost with other methods for CO₂ Capture and Storage and CO₂ supplies to greenhouses.

1.5 Organization of the thesis

This thesis consists of six chapters. Chapter 1 gives an introduction of greenhouse gas emissions and controls, the background of CO₂ enrichment in greenhouses, the concept of CO₂ capture from air and its application in greenhouses, and the research objectives of the proposed study. Chapter 2 presents a literature review on reported methods for CO₂ capture from air and the performance of 13X zeolite adsorbent for CO₂ adsorption. The experimental set-up and procedures are described in Chapter 3. The relevant experimental results are presented and discussed in Chapter 4. In Chapter 5, an economic analysis on proposed method is conducted. Finally, Chapter 6 draws the conclusions, and provides recommendations for the future work.

Chapter 2 Literature review

Carbon capture and storage (CCS), also known as carbon capture and sequestration, refers to the technology to capture carbon dioxide from large point sources, with the aim of preventing large amount of CO₂ from entering the atmosphere. In general, CCS consists of three processes, as illustrated in Figure 2-1: (1) capturing CO₂ from emission sources, (2) compression and transporting CO₂ to a proper storage site, (3) depositing CO₂ permanently so that it won't be released to the atmosphere, such as terrestrial, subterranean, and oceanic locations[20].

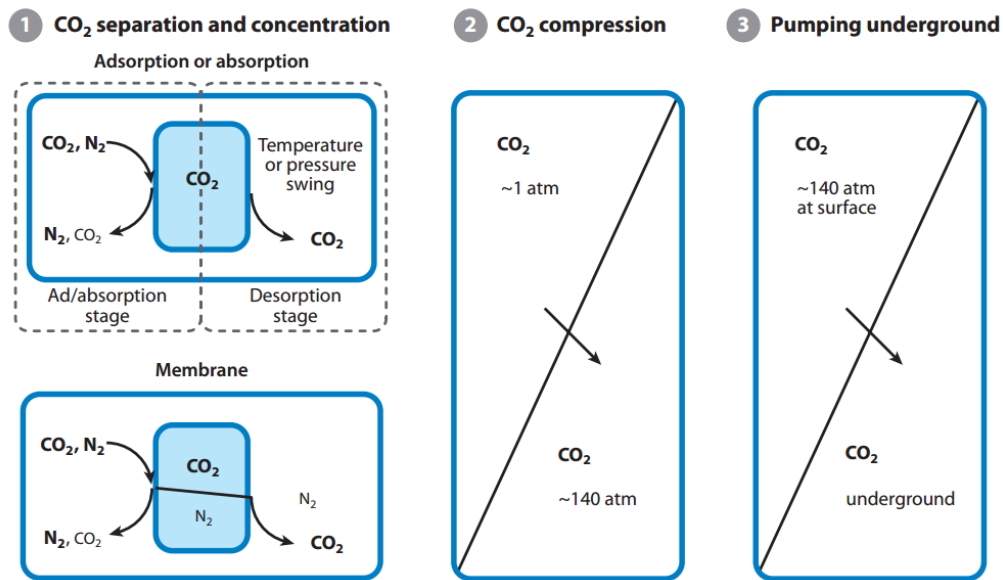


Figure 2-1 Three steps in CCS[20]

CO₂ is commonly captured from the flue gases of fossil-fuel burning power plants after it is generated from the combustion of fossil fuels, in which a regenerable liquid solvent is applied. This is called “post-combustion capture”. Another method named “pre-combustion capture” refers to removing CO₂ from fossil fuels before the fuel is completely combusted. The fossil fuel is first converted to syngas (CO+H₂), which is further upgraded to Hydrogen and CO₂ by water-

shift reaction. CO₂ is then separated from H₂ before H₂ is combusted or oxidized. The resulting CO₂ can be captured from a relatively pure exhaust stream. The third option, “oxy-fuel combustion”, denotes the technology to burn fuels with pure oxygen instead of air, leading to a high CO₂ concentration that can be directly compressed.

After capturing, CO₂ will be transported to storage sites usually by pipelines. Those places might be oil production fields where CO₂ is injected into the older fields for enhanced oil recovery. CO₂ can be permanently stored in many forms, including geological storage, ocean storage, and mineral storage, all aiming at locking up CO₂ for thousands of years.

Among these three steps in CCS, the first step, CO₂ capturing, accounts for most of the cost by approximately 75% [20]. Therefore, researchers have focused on developing more efficient and cost-effective capture technologies.

2.1 Capturing CO₂ directly from ambient air

The main target of carbon capture and storage is to reduce carbon dioxide emissions by capturing CO₂ and putting it into secure storage. However, most proposed methods are dealing with the carbon dioxide emitted from large point sources that contain relatively high concentrations of CO₂.

Based on the results given by United States Environmental Protection Agency (US-EPA), global greenhouse gas emissions can be broken down by the economic activities that lead to their production [21]. Figure 2-2 represents the distribution of these emissions by sources.

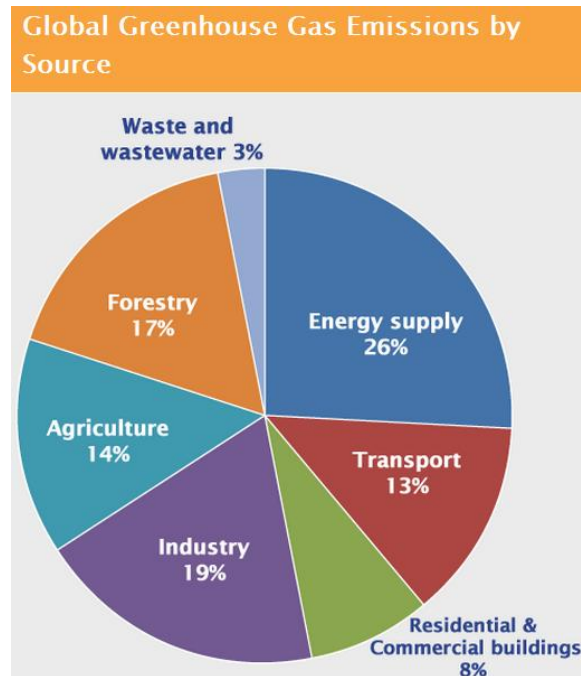


Figure 2-2 Global greenhouse gas emissions by sources[21]

Emissions from industry and energy supply only account for 19% and 26% of total emissions respectively. These emissions are produced mostly from large power plants by burning fossil fuels, which contain concentrated CO₂. Agriculture accounts for 14% of total emissions, mostly from the management of agricultural soils, livestock, and crop production. Fossil fuels burned for land, air and marine transportation also contribute to greenhouse gas emissions by 13%. Forestry emits carbon dioxide from deforestation, land clearing, and fires or decay of peat soils, which is 17% of total emissions. Emissions from forestry, agriculture, transportation and residential buildings are usually distributed sources, especially from transportation, making them difficult to be captured. Therefore, direct CO₂ capture from the ambient air seems necessary.

In 1999, Lackner[8, 22] first proposed the concept of “air capture” as an approach to mitigate carbon dioxide emissions. Compared with traditional carbon dioxide capture approaches, direct capture from the air displays some apparent advantages.

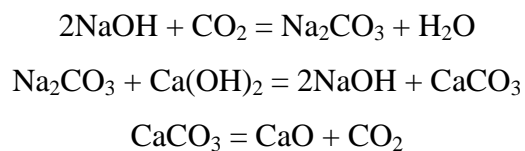
- 1) It deals with all sources of CO₂ and it even could be scaled up to reduce current levels of atmospheric CO₂.
- 2) Air capture can play a role in the reduction of greenhouse gas emissions without making the existing energy or transportation infrastructure useless [23].
- 3) There would be no requirement for the construction of pipelines to transport CO₂ to secure storage and reduce the risk of CO₂ leakage from geological storage[24].

If direct capture of CO₂ from the ambient air is successfully operated on a large scale, it will definitely provide an alternative to reduce global carbon emissions. However, removal of CO₂ from the ambient air is still in the early stage and just started to gain more attentions recently.

2.1.1 CO₂ capture from air by absorption and adsorption

The history of extracting CO₂ from dilute sources can be dated back to the 1940s and 1950s, while fundamental absorption processes were proposed [25-27].

Zeman & Lackner[28] proposed a method of carbon capture from the atmosphere using dissolved sodium hydroxide to absorb CO₂ from the ambient air. The resultant sodium carbonate solution was then causticized by calcium hydroxide to regenerate the sodium hydroxide solution and produce calcium carbonate, a famous process named Kraft Process. The calcite was thereafter thermally decomposed to produce lime and CO₂, driving off a concentrated CO₂ stream for recovery [20, 28]. Reactions involved in the process are listed as follows:



Results showed that the proposed process was well defined and technically feasible.

Keith [29] has also proposed a process for air capture using sodium hydroxide. Figure 2-3 shows the sodium hydroxide air capture system. In the absorber or contactor, sodium carbonate was produced by the contact of the sodium hydroxide solution with the ambient air. Then the resultant solution containing carbonate was sent to the Causticizer. In the Causticizer, lime (CaO) was added to the solution, producing solid calcium carbonate and sodium hydroxide. Then precipitated CaCO_3 was sent to the Calciner while NaOH was delivered back to the Contactor to absorb CO_2 . In the Calciner, CaCO_3 was heated and decomposed to lime again, finally releasing CO_2 from the system.

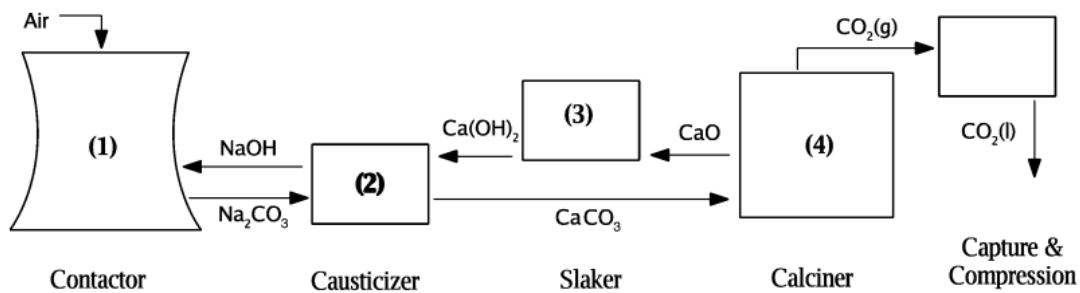


Figure 2-3 Sodium hydroxide air capture system[29]

In 2006, Mazzotti[30] proposed a detailed process design with a packed column contactor, based on the scheme of existing technologies of Lackner, including CO_2 absorption, carbonate precipitation, sludge dewatering train, calcinations, slaking, oxygen purification, and CO_2 compression. However it was pointed out by the author that the specific energy demand of 17 GJ/t- CO_2 was larger than the heat released to emit the same amount of CO_2 by the combustion of coal (9 GJ/t- CO_2), and smaller than that of methane (20 GJ/t- CO_2)[20, 30]. It is obvious that burning fossil fuels to provide the energy required by the capture process doesn't seem to be a wise route as it goes against the primary goal of reducing the carbon dioxide emissions. Therefore the feasibility of removal CO_2 from the air by aqueous alkaline solution was questionable.

In order to improve the existing design, Keith[31] came up with a prototype contactor with a sodium hydroxide spray tower instead of the previously mentioned packed bed column. The prototype showed the feasibility of this capturing process based on the detailed material and energy requirements analyses. The diagram of the prototype contactor in such a process is shown in Figure 2-4. CO₂ from the ambient air was absorbed by sodium hydroxide spray. CO₂ concentration at the inlet and outlet was detected and the rate of CO₂ absorption was calculated based on mass transfer. Later they developed a direct sodium tri-titanate causticization pathway to replace the traditional lime causticization method[32], reducing the heat requirement in sodium hydroxide regeneration process by half by lowering the regeneration temperature.

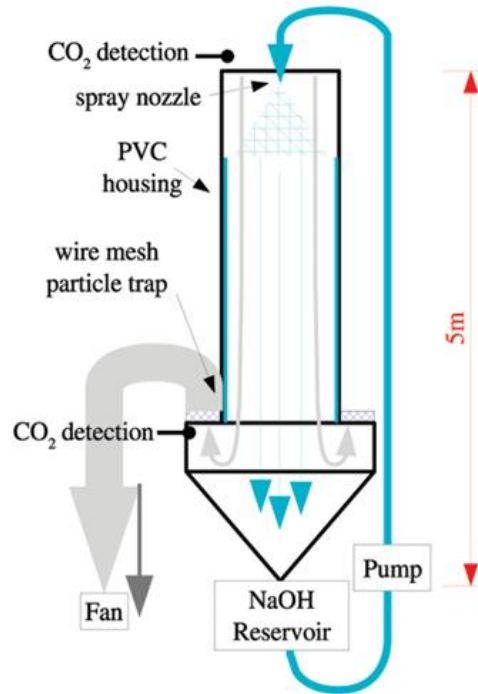


Figure 2-4 Diagram of prototype contactor[31]

Despite of the widely developed approaches to capture carbon dioxide from the air by aqueous solutions, there exists a significant drawback in all these processes. The regeneration process is multi-stage and energy intensive [33]. After CO₂ was absorbed by the alkaline solution, calcium

carbonate was formed and it should be recovered by calcinations, releasing a concentrated CO₂ stream [34]. However, calcination is the most energy intensive stage due to the high temperature required to break the strong calcium carbonate bond, usually more than 900 °C. A recent study on the feasibility of capturing CO₂ directly from the ambient air by American Physical Society pointed out that CO₂ absorption by aqueous solution was economically unfeasible [35].

High energy requirements, corrosiveness of strong alkaline solutions, and difficulty in regeneration process lead to the exploration of solid sorbents in capturing CO₂ from the ambient air by adsorption [36].

The chemisorptions of CO₂ on solid sorbents have been reported by Steinberg's group [37, 38]. The process was accomplished by consecutive CaO-carbonation and CaCO₃-calcination cycles in a fluidized-bed solar reactor [37]. They further studied the thermodynamics and thermogravimetric analysis of three different Na-based thermochemical cycles[39]. It was found that the carbonation of solid NaOH at 25 °C with dilute CO₂ source of 500 ppm was quite slow, reaching just 9% after 4 hr. What's more, the thermal decomposition of NaHCO₃ and Na₂CO₃ took place at 90-200 °C and 1000-1400 °C respectively. The low carbonation rate and high energy intensity made this process unfeasible both technically and economically [2].

Composites “K₂CO₃ in porous γ -Al₂O₃” were reported to be promising sorbents to capture CO₂ from flue gases [40-43]. It was applied by Veselovskaya [33] to capture CO₂ directly from the air via temperature swing adsorption. The adsorption and regeneration experiments using air were conducted in a continuous-flow system. Adsorption capacity and thermal stability were studied. It was shown that CO₂ adsorption capacity was 23 ml-CO₂/g-sorbent when regeneration temperature was set at 300 °C, with an increase of 40% in capacity when regenerated at 150 °C. The stability of the sorbent has been evaluated well over 80 cycles.

Moisture swing provides a new option to capture CO₂ and regenerate the sorbent. It was reported by Wang[7] that an amine-based anion exchange resin can be applied as a sorbent for moisture

swing adsorption. The resin was dispersed in a flat sheet of polypropylene in alkaline forms so that it was able to adsorb carbon dioxide from the air. The ammonium cations were attached to the polymer structure, and the hydroxide and carbonate behaved as dissociative anions. The resin could adsorb carbon dioxide under dry conditions and CO_2 would be desorbed when the resin was wetted. The process was illustrated in Figure 2-5. The adsorption isotherm has proved that the resin behaves well even dealing with ultra-low CO_2 concentrations, with an adsorption capacity of 0.86 mol CO_2 per kilogram of resin at 25 °C [44]. Humidity effect was also evaluated later and the results indicated that humidity would have a strong influence on the adsorption equilibrium at room temperature[7].

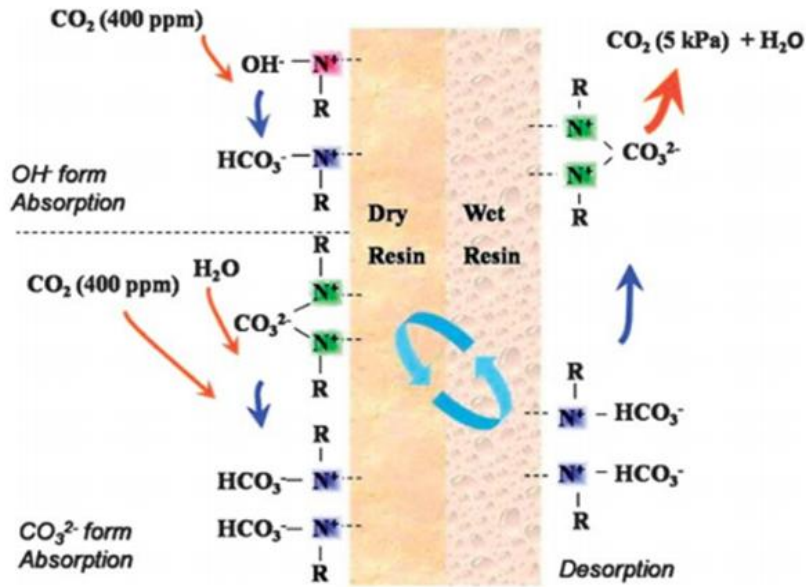


Figure 2-5 Moisture swing adsorption of CO_2 on a quaternary ammonium functionalized ion exchange membrane [7]

2.1.2 Different methods for CO₂ capture from air by adsorption

Compared with other approaches for CO₂ removal, adsorption is recognized to be an energy-efficient, cost-effective option[45]. One of the challenges researchers are facing while developing the technology to directly capture CO₂ from the ambient air is to identify the proper adsorbents that have high adsorption capacity when dealing with gases of very low CO₂ concentrations, i.e. 400 ppm in ambient air. An ideal adsorbent for capturing CO₂ should have the following characteristics: (1) high CO₂ adsorption capacity, (2) high adsorption selectivity toward CO₂ against other gases (e.g. N₂ and moisture), (3) low energy requirements for regeneration, (4) stability to prolonged adsorption-desorption cycling, and (5) tolerance to the presence of moisture [46].

Depending on the characters of various adsorbents, solid-gas adsorption operations may be carried out via two modes. One is isothermal regeneration mode, also called pressure swing adsorption (PSA). The other one is non-isothermal regeneration mode, such as temperature swing adsorption (TSA) [47]. These two modes are operated by controlling the pressure or temperature. In PSA, adsorption and desorption take place by pressurization and depressurization, alternately. While in TSA, adsorption takes place at lower temperature and desorption occurs when temperature is increased.

Many types of adsorbents have been reported to be capable of adsorbing CO₂, including zeolites[48-52], activated carbon[50, 53, 54], metal organic frameworks (MOF)[55-57], etc.. Solid adsorbents based on supported amines have been explored recently, and they show promising CO₂ adsorption performances. Depending on the interaction between support and active sorbent and the method used in the preparation of the adsorbent, supported amine adsorbents can be further divided into three classes[58], as shown in Figure 2-6. Class 1 adsorbents are based on porous supports (usually silica) impregnated with monomeric or polymeric amines. This class was studied by Song in 2002 [59-61]. Class 2 adsorbents are based on amines that are covalently linked to a solid support, where amines are bounded to oxides to

ensure the permanent immobilization of the active compounds [2]. Tsuda [62, 63] first evaluated the class 2 adsorbents in 1992, and Sayari's group has been extensively studying this class of adsorbents [64-70]. Class 3 adsorbents are those where aminopolymers are polymerized in the porous support materials, and they were first reported by Jones' group in 2008[71].

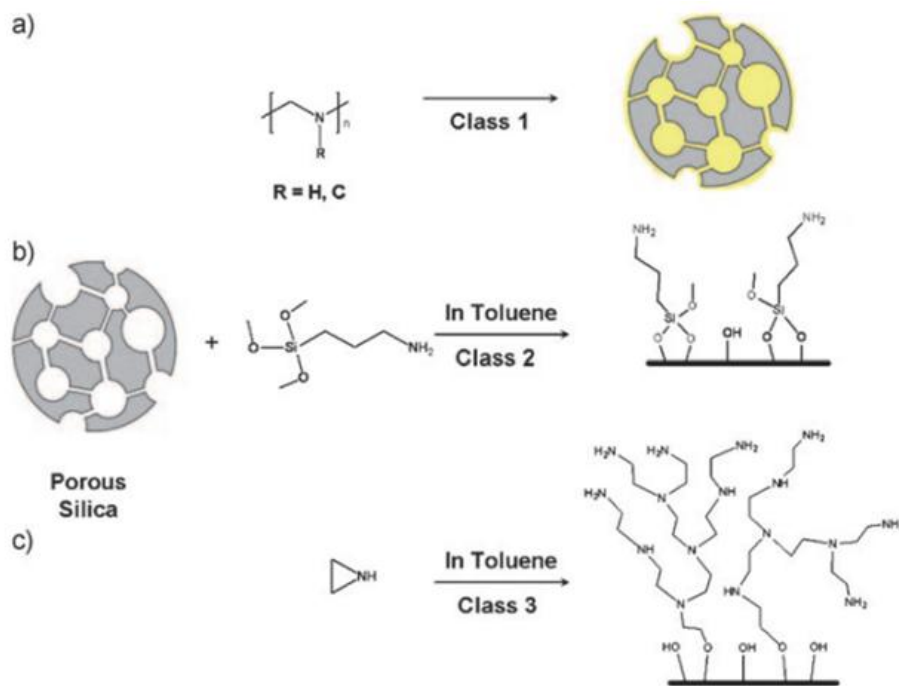


Figure 2-6 Classification of supported amine adsorbents [58]

Class 1 adsorbents:

Solid materials based on fumed silica impregnated with polyethylenimine (PEI) were proved to be superior adsorbents for capturing carbon dioxide from the atmosphere[72]. PEI was coated on the surface of fumed silica (FS), named FS-PEI. Goeppert [62] showed that FS-PEI had an adsorption capacity of 1.74 mol-CO₂/kg directly from the ambient air at 25 °C even under humid conditions.

Choi[6, 73] also developed modified PEI-based aminosilica adsorbents, derived from PEI

modified with 3-aminopropyltrimethoxysilane (A-PEI/silica) or tetraethyl orthotitanate (T-PEI/silica), and applied them for the capture of carbon dioxide from air. The modified adsorbents were shown to have an enhanced adsorption capacity of more than 2 mol-CO₂/kg, and were very stable over the adsorption-desorption cycles even in the presence of moisture.

Class 2 adsorbents:

It was first reported by Sayari[67] that an amine-functionalized silica, triamine-functionalized pore-expanded mesoporous silica (TRI-PE-MCM-41), could be applied for the CO₂ adsorption from dry and humid air. The adsorption isotherm for dry CO₂ was evaluated at 25 °C up to 0.05 bar. Column-breakthrough measurements were also performed to demonstrate the high selectivity toward CO₂ in the presence of N₂ and O₂. The obtained adsorption capacity was 0.98 mol-CO₂/kg at a CO₂ concentration of 400 ppm.

Class 3 adsorbents:

Another amine-based solid adsorbent, hyperbranched aminosilica (HAS), was evaluated by Jones[73] for direct CO₂ capture from ambient air. It was synthesized via in-situ ring-opening polymerization of aziridine off porous solid supports[71]. The adsorption performance of HAS was assessed under humid conditions in a fixed bed unit with 400 ppm CO₂ in the test gas. Results showed that HAS had an adsorption capacity of 1.72 mol-CO₂/kg at ambient conditions. On the other hand, the stability tests demonstrated its tolerance to repeated temperature swing cycles.

2.2 13X zeolite for CO₂ adsorption

A survey of the vast patent literature shows that the most widely used adsorbent for CO₂ removal by pressure swing adsorption and temperature swing adsorption is molecular sieve zeolite, such as 13X zeolite (also known as NaX) [48, 74-77].

Rege[77] studied the adsorption isotherms and kinetics of the common air impurities including CO_2 , H_2O and CH_4 on commercial 13X zeolite and other adsorbents over a wide concentration range. The adsorption isotherm of CO_2 revealed that 13X zeolite had the highest adsorption capacity over natural zeolite clinoptilolite and $\gamma\text{-Al}_2\text{O}_3$ at ppm levels of CO_2 , as shown in Figure 2-7. The high capacity makes 13X an ideal adsorbent to be utilized in a temperature swing adsorption process.

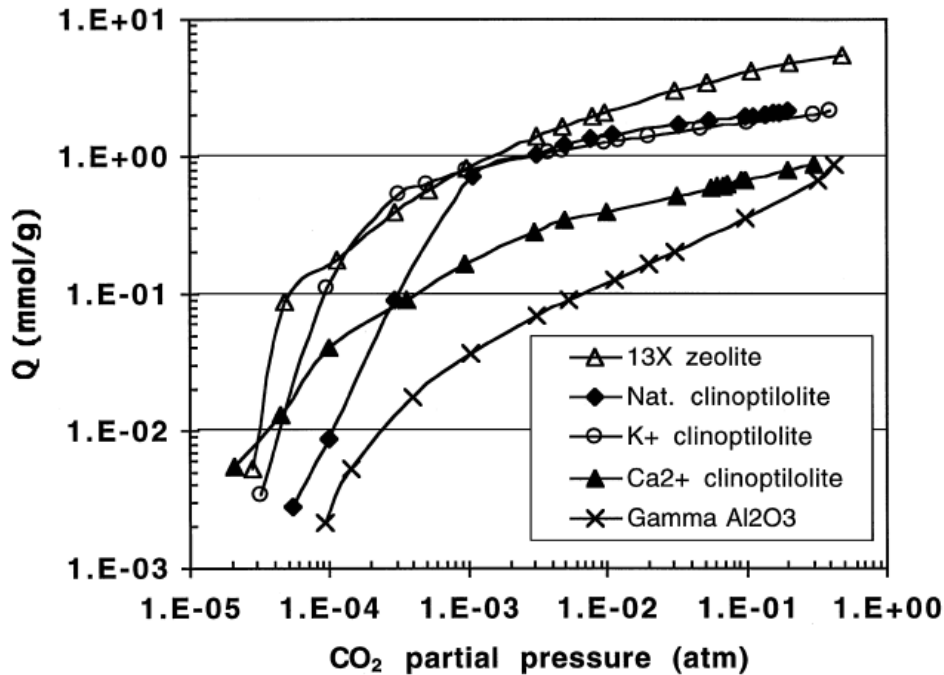


Figure 2-7 Adsorption isotherm of CO_2 on different sorbents at 295 K[77]

Siriwardane[51] also evaluated the adsorption of CO_2 on zeolites including 4A, 5A and 13X at moderate temperatures. Similar to Rege's work, it was clearly seen from the adsorption isotherms of CO_2 at 120 °C that 13X zeolite outperformed others, giving the highest adsorption capacity of 0.7 mol/kg at a CO_2 partial pressure of 1 atm. As for the regenerability, the adsorption capacity of zeolites can be fully recovered after regeneration at 350 °C.

The removal of CO_2 by adsorption with 13X zeolite has also been investigated by Konduru [78].

Five adsorption and desorption cycles were carried out with an inlet CO₂ concentration of 1.5% at standard conditions. Temperature swing adsorption was employed and the adsorbent was regenerated at 135 °C. The adsorption capacity was 1.77 g-CO₂/kg-sorbent, and decreased to 1.36 g-CO₂/kg-sorbent after five cycles.

An indirect temperature swing adsorption process for CO₂ removal from N₂ using 13X zeolite was studied by Merel [79]. A column made of two concentric tubes was used for the adsorption and desorption tests. The internal tube was designed as a heat exchanger to provide heat to 13X by means of steam condensation and to cool it down via circulating water, in which temperature swing adsorption was completed. The annulus formed by the inner tube was loaded with 13X where adsorption and desorption took place. Both non-cyclic experiment and cyclic experiments were carried out, and breakthrough curves were obtained.

Zhao[80] developed a modified 13X zeolite for adsorption of carbon dioxide. The shaped 13X zeolite was hydrothermally modified with kaolin as binder to improve the adsorption performance. Compared with the commercial 13X zeolite, the modified adsorbent exhibited higher adsorption capacity and carbon dioxide uptake rate. This can be explained by the increase of effective adsorption surface area and the decrease of diffusion resistance as kaolin binder was converted into the zeolite.

A dual-column temperature and vacuum swing adsorption with 13X zeolite was conducted by Su[81] to study the adsorption of CO₂ from a gas stream. The regenerability of 13X zeolite has been proved by more than 100 cycles of temperature and vacuum swing adsorption experiments. 13X zeolite was less influenced by the presence of moisture below 30°C and presented stable adsorption behaviour under humid conditions. These results suggest that 13X zeolite is a promising adsorbent for CO₂ capture.

Most of the researches have focused their researches on the adsorption of CO₂ by 13X zeolite for gases of relatively high CO₂ concentrations, and the adsorption for gases of ultra-dilute CO₂, the

ambient air for instance, is still in its infancy. Figure 2-8[47] and Figure 2-9[82] show the CO₂ adsorption isotherms on various adsorbents. At the lowest CO₂ partial pressure as tested, 13X outperformed all other adsorbents, exhibiting the highest adsorption capacities.

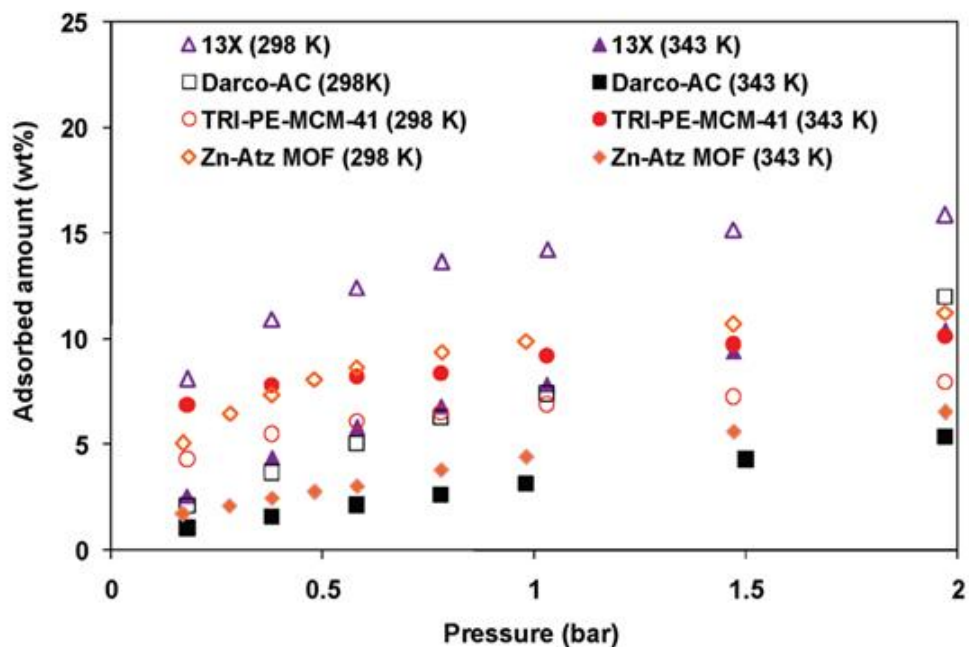


Figure 2-8 Adsorption isotherms of CO₂ on various adsorbents [47]

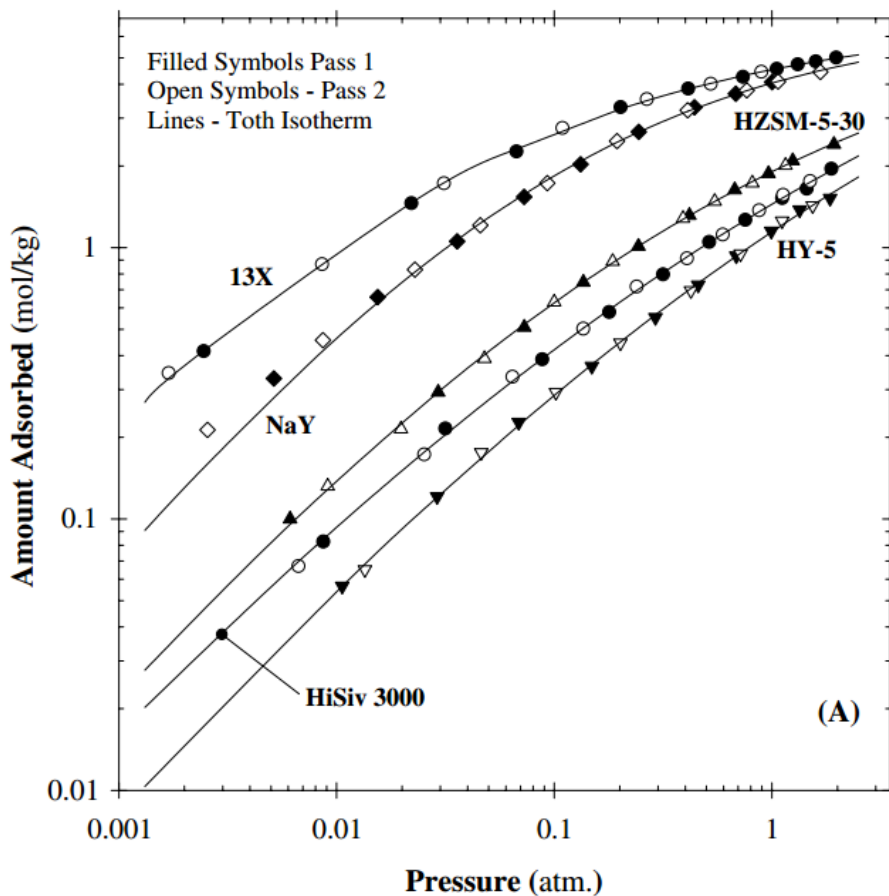


Figure 2-9 Carbon dioxide adsorption isotherms on various adsorbents [82]

Wang [83] conducted experiments on adsorption of CO₂ at low concentrations by zeolites, with the CO₂ adsorption isotherms at 333K being shown in Figure 2-10. At the lowest CO₂ partial pressure of 0.004 kPa, 13X zeolite had an adsorption capacity of 4 cc-STP/g, equivalent to 0.178 mol-CO₂/kg-sorbent.

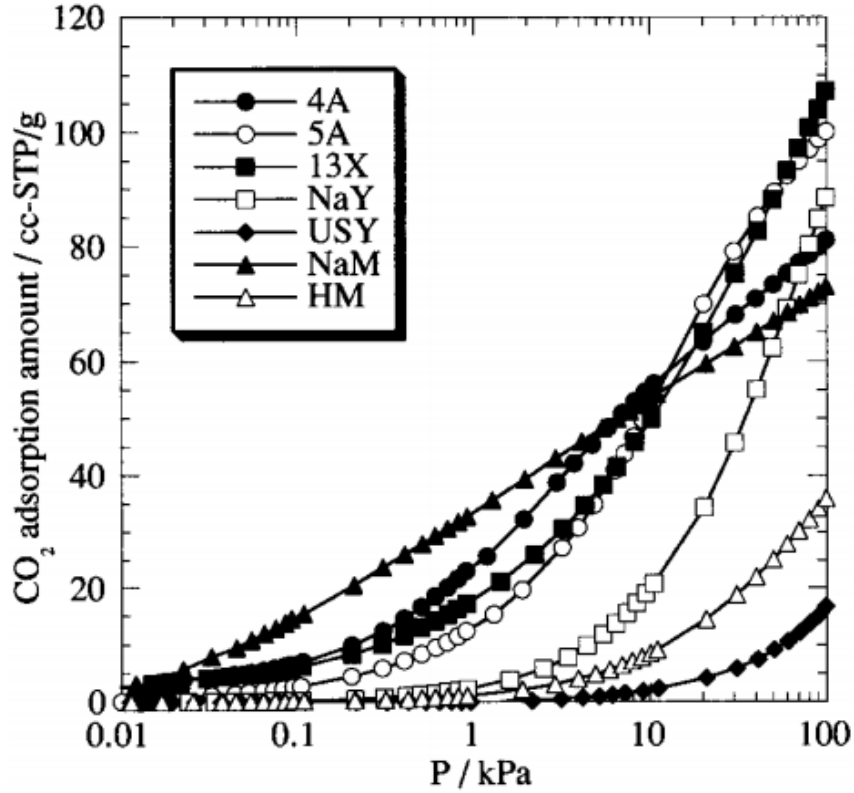


Figure 2-10 CO₂ adsorption isotherms at 333K [83]

The adsorption capacity can also be estimated based on reported adsorption models. Kamiuto[84] studied CO₂ adsorption by 13X at relatively low CO₂ partial pressures. A Langmuir equilibrium adsorption capacity equation was developed by fitting their experimental data, which relates the amount of CO₂ adsorbed q (kg-CO₂/kg-bed) to the CO₂ concentration C (kg-CO₂/m³),

$$q = bC/(1 + aC) \quad (2-1)$$

where $\ln a = 9.625 - 0.0244T$ and $\ln b = 9.840 - 0.0319T$ for 13X zeolite. The adsorption capacity of 13X zeolite for 400 ppm CO₂ in ambient air at 25 °C was estimated to be 0.025 mol-CO₂/kg sorbent from the above equation. They also fitted their data to the Dubinin-Astakhov equation,

$$\frac{q}{\rho^*(T)} = w \exp \left[- \left(\frac{A}{E} \right)^n \right] \quad (2-2)$$

where w (m³/kg-bed), E (kJ/mol) and n are adjustable parameters and $n=2.28$, $w=1.63 \times 10^{-4}$ and $E=18.7$ for 13X zeolite. The adsorption capacity was estimated from this equation to be 0.16 mol-CO₂/kg sorbent for ambient air at 25 °C with 400 ppm CO₂.

In summary, a literature review identifies both amine-supported sorbents and zeolite-based sorbents (13X) as potentially applicable for enriching CO₂ concentration from 400 to 1000 ppm in ambient air so as to use the enriched stream to provide CO₂ for greenhouses. While amine-supported sorbents delivered a superior performance on CO₂ capture from ambient air, it is still under development and potentially quite expensive. 13X zeolite, a widely used commercial sorbent, possesses a high adsorption capacity, good regenerability, and reasonable tolerance to moisture, which make 13X zeolite a promising candidate for adsorbing CO₂ directly from the ambient air. Due to the lack of performance data at extremely low CO₂ concentrations in the literature, experiments will be carried in this study to evaluate the performance of selected 13X sorbent for CO₂ enrichment using ambient air.

Chapter 3 Experimental setup and procedures

3.1 Materials and methods

3.1.1 Materials

Commercially available zeolite 13X was selected as the adsorbent for CO₂ adsorption and desorption due to its reported high adsorption capacity and wide usage for CO₂ gas separation. Spherical 13X particles with a mean diameter of 3.9 mm and a bulk density of 0.7 g/ml were purchased from Shanghai Molecular Sieve Co., Ltd. The BET surface area, pore volume and pore size of zeolite 13X were 321 m²/g, 0.12 cm³/g and 14.89 nm, respectively. Before the adsorption experiments, 13X was dried in the oven at 110 °C for 12 hr to remove the moisture.

The CO₂/N₂ gas cylinder was obtained from Praxair, which contains 1000 ppm CO₂ balance with N₂. Gas streams containing lower CO₂ concentrations were prepared by mixing pure N₂ and 1000 ppm CO₂.

3.1.2 Methods

Both temperature swing adsorption and pressure swing adsorption have been commonly used for purification of gas mixtures. In the following experiments, temperature swing adsorption was selected in view of that heat is readily available in most greenhouses and the operation is simpler than pressure swing operation.

CO₂ concentrations of the effluent gas stream were detected by a CO₂ analyzer, Model 906 from Quantek Instrument, as shown in Figure 3-1. The analyzer contains a solid-state infrared sensor for the measurement, and can record CO₂ concentration continuously during the experiments. The accuracy of the instrument is +/- 1% of reading.



Figure 3-1 Model 906 CO₂ analyzer

3.2 Experimental setup and procedures

The CO₂ adsorption and desorption process diagram is shown in Figure 3-2. The column was made of glass with a water jacket surrounding the column. The column was 1 ft high with an internal diameter of ¼ in for gas to flow through. The water jacket was used to maintain the column at desired adsorption (T_{ad}) or desorption temperature (T_{de}), controlled by two water baths separately. Two rotameters were used to control the input CO₂ concentration (C_{in}) by regulating the flow rates of two gas streams which were pure N₂ and 1000 ppm CO₂ balanced with N₂. The input gas flowed into the inner column packed with adsorbent where adsorption and desorption took place, with outlet CO₂ concentration (C_{out}) being measured by the in-situ CO₂ analyzer.

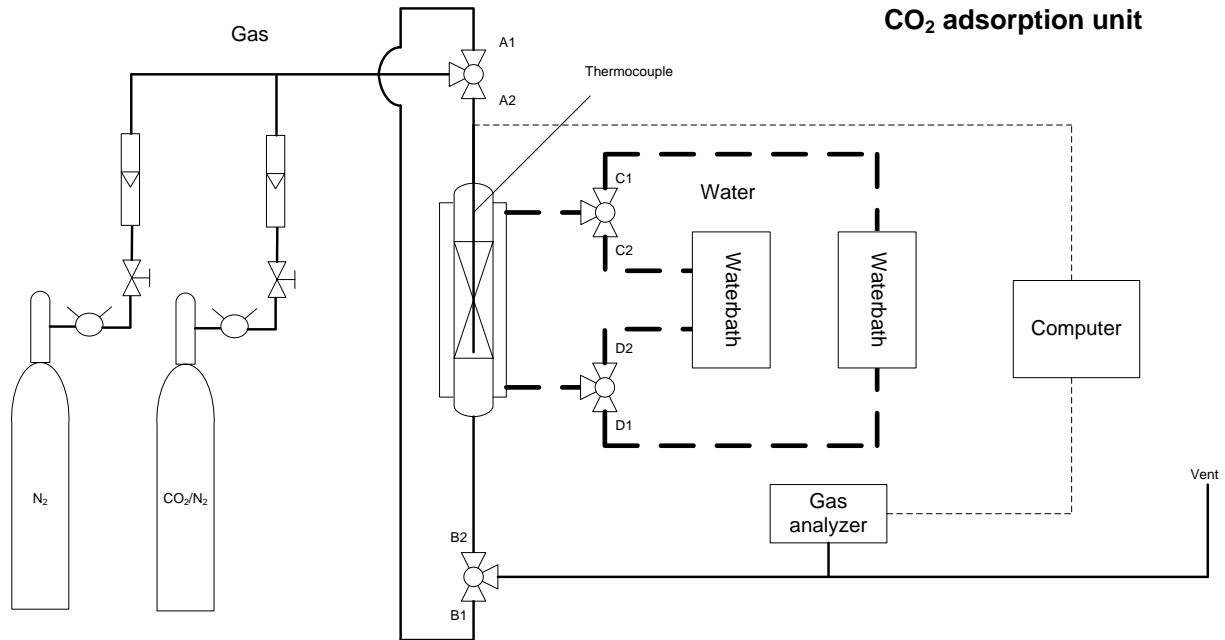


Figure 3-2 Process diagram of CO₂ adsorption and desorption unit

The whole unit setup is illustrated in Figure 3-3. Adsorbents were first loaded into the inner column. The gas mixture was cooled down to desired T_{ad} via passing through the water bath before flowed into the inner column. CO₂ in the gas mixture would be gradually adsorbed by the adsorbent, with the CO₂ concentration in the gas mixture exiting the bottom of the column being monitored by the CO₂ analyzer continuously. When adsorption was completed, the unit was switched to desorption mode by quickly increasing the temperature of the column via switching the water passing through the jacket from the low temperature water bath to the high temperature water bath. With the same gas stream at a higher temperature, the adsorbed CO₂ during adsorption period would desorb from adsorbent into the passing gas mixture. As a result, the gas stream exiting the column would contain more CO₂ than the inlet, leading to a CO₂-enriched gas stream which can be pumped into the greenhouse to stimulate plant growth.

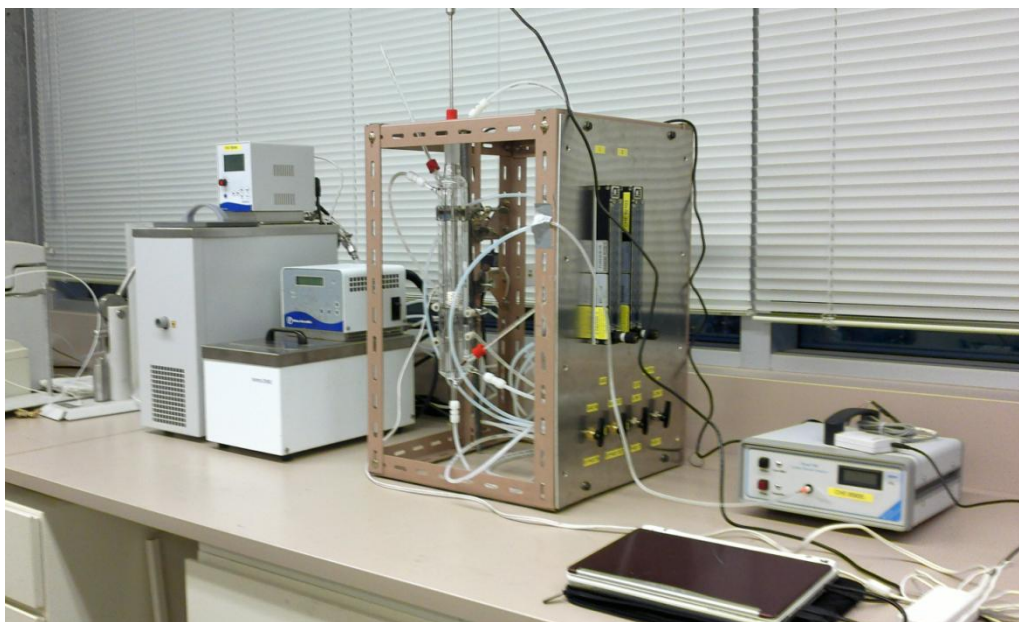


Figure 3-3 CO₂ adsorption and desorption unit

A typical adsorption and desorption curve recorded by the analyzer is shown in Figure 3-4. At the beginning of adsorption, CO₂ was quickly adsorbed by the adsorbent as indicated by the near zero CO₂ concentration in the effluent stream. After this initial adsorption period, the adsorbent started to get saturated layer by layer, accompanied by a gradual increase in CO₂ concentration in the outlet gas until a complete saturation was reached when a concentration approached the inlet CO₂ concentration. As the temperature increased abruptly, the adsorbed CO₂ started to be desorbed from the adsorbent. The concentration reached a peak and then gradually dropped down to the initial base level. The integration of part A would give the amount of CO₂ adsorbed, and the integration of part B would provide the amount of CO₂ desorbed.

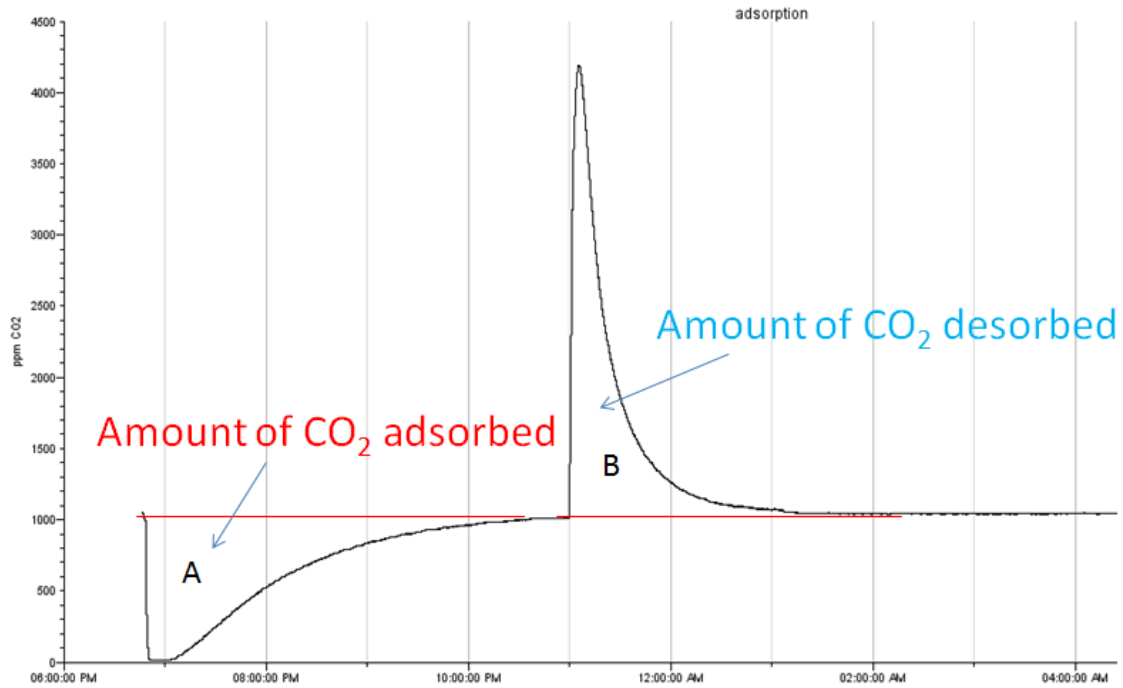


Figure 3-4 Adsorption of CO₂ from 1000 ppm CO₂ and balanced N₂ gas mixture at 10°C and desorption at 30 °C

The inlet gas flow rate (Q_{in}) was controlled at 1 L/min and outlet flow rate (Q_{out}) was analyzed in the following section. The CO₂ adsorption capacity (q_{ad}) and desorption capacity (q_{de}) were defined as

$$q_{ad} = \frac{1}{M} (Q_{in} C_{in} t_{ad} - \int_0^{t_{ad}} Q_{out} C_{out} dt) \quad (3-1)$$

and

$$q_{de} = \frac{1}{M} \left(\int_0^{t_{de}} Q_{out} C_{out} dt - Q_{in} C_{in} t_{de} \right) \quad (3-2)$$

where M is the adsorbent loading, t_{ad} and t_{de} are adsorption and desorption time.

A moving average concentration at a certain time t after desorption begins is estimated as

$$c(\text{ave}) = \frac{\int_0^t C_{\text{out}} dt}{t} \quad (3-3)$$

An enrichment factor (f) is defined to describe how many times CO_2 concentration is increased over its initial inlet value

$$f = \frac{c(\text{ave})}{c_{\text{in}}} \quad (3-4)$$

Chapter 4 Experimental results and discussions

The whole experiments are divided into four sections. First, the influence of desorption flow rates was investigated to identify the most effective desorption flow rate. Secondly, preliminary experiments on 1000 ppm CO₂ were carried out to examine the general performance of 13X adsorbent. Then experiments were carried out with the gas mixture with 400 ppm CO₂, typical CO₂ concentration in atmospheric air, to systematically evaluate the feasibility of CO₂ enrichment from ambient to desirable 1000 ppm level. Finally, moisture effects on the performance of 13X were studied to assess the performance under real atmospheric conditions.

4.1 Influence of desorption flow rate

4.1.1 Purpose

The performance of CO₂ enrichment is determined by several variables, which include adsorbent loading, inlet CO₂ concentration, adsorption temperature, adsorption flow rate, desorption temperature and desorption flow rate. Among those variables, different adsorbent loadings, adsorption temperatures and desorption temperatures will lead to different adsorption and desorption capacities. When inlet CO₂ concentration and flow rate at adsorption stage are fixed at certain values, the only variable that affects the experimental performance, like the enrichment factor, is the desorption flow rate at each given desorption temperature. Therefore, the purpose here is to identify the most effective desorption flow rate.

4.1.2 Experimental conditions

Three sets of experiments were conducted with adsorbent loadings of 5 g, 10 g and 20 g, respectively. Inlet CO₂ concentration was set at 1000 ppm, and adsorption flow rate was 1 L/min.

In each experiment, adsorption and desorption temperatures were fixed at 20 °C and 50 °C respectively. Desorption flow rate varied from 0.2 L/min to 1 L/min.

4.1.3 Results and discussions

The results are given in Figure 4-1, Figure 4-2 and Figure 4-3, reporting the moving average concentrations with 5 g, 10 g, and 20 g adsorbent loadings, respectively, at different desorption flow rates. Although the initial CO₂ concentration was set to 1000 ppm, the initial CO₂ concentration was seen to be slightly below 1000 ppm, which was a result of the baseline drift of CO₂ gas analyzer.

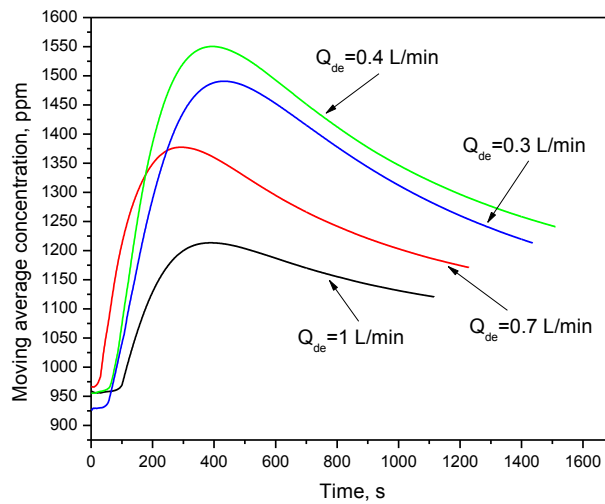


Figure 4-1 Moving average concentrations with an adsorbent loading of 5 g

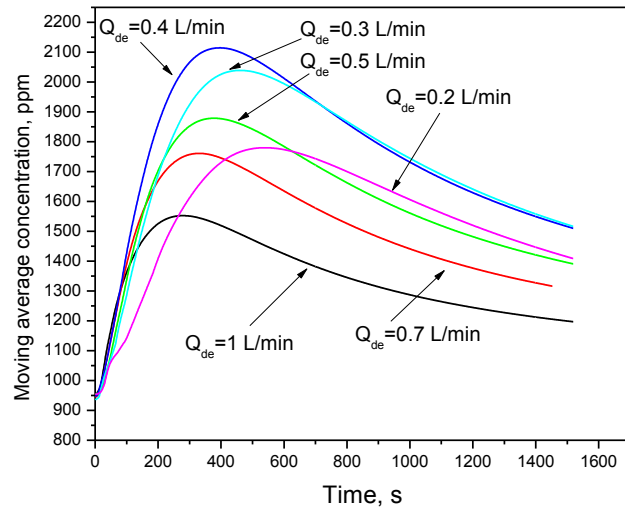


Figure 4-2 Moving average concentrations with an adsorbent loading of 10 g

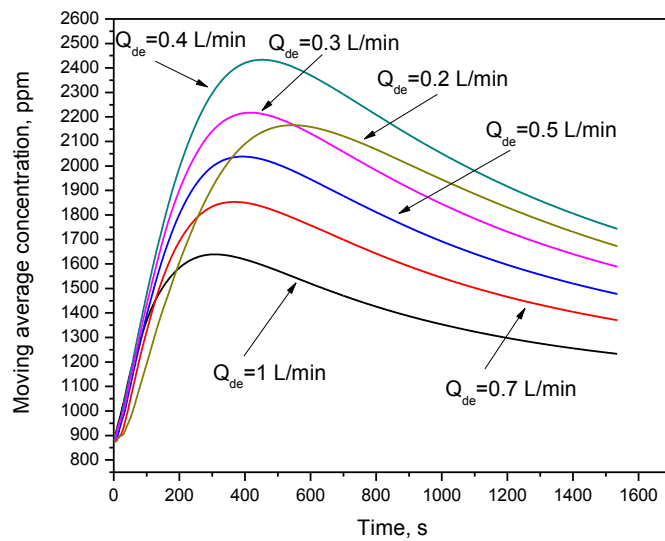


Figure 4-3 Moving average concentrations with an adsorbent loading of 20 g

The curves in all three figures show that when the desorption flow rate decreased from 1 L/min to 0.4 L/min, the moving average concentrations became higher and higher, meaning that there was a higher potential for CO₂ enrichment in the outlet stream. In contrary, when desorption flow rates were further decreased to 0.2 L/min, the CO₂ concentration in outlet stream became lower. The desorption flow rate of 0.4 L/min thus defined the transition point. For each single curve, the moving average CO₂ concentration always increased first to a peak and then dropped as desorption rate slowed down.

This can be explained by the definition of moving average concentration:

$$\text{Moving average concentration} = \frac{\text{Amount of CO}_2 \text{ desorbed}}{\text{Desorption flowrate} * \text{Time}} \quad (4-1)$$

For a given CO₂ desorption rate, the smaller desorption flow rate leads to a higher moving average concentration. However the mass transfer of CO₂ between the flowing gas and solid adsorbent can be influenced by the gas flow rate. As the flow rate decreases, mass transfer between two phases becomes worse. As a compromise, an optimal flow rate may exist at which the moving average concentration is maximized. According to the results in Figure 4-1, Figure 4-2 and Figure 4-3, the optimal desorption flow rate was around 0.4 L/min because the moving average CO₂ concentrations was higher than almost all others. This can be seen more clearly in Figure 4-4 when the peak concentrations are plotted as a function of desorption gas flow rates. For 5 g, 10 g, and 20 g adsorbent loadings, a desorption flowrate of 0.4 L/min gives the highest peak moving-average concentration. It can thus be concluded that the most effective desorption concentration for 13X is about 0.4 L/min when the adsorption flow rate is kept at 1 L/min.

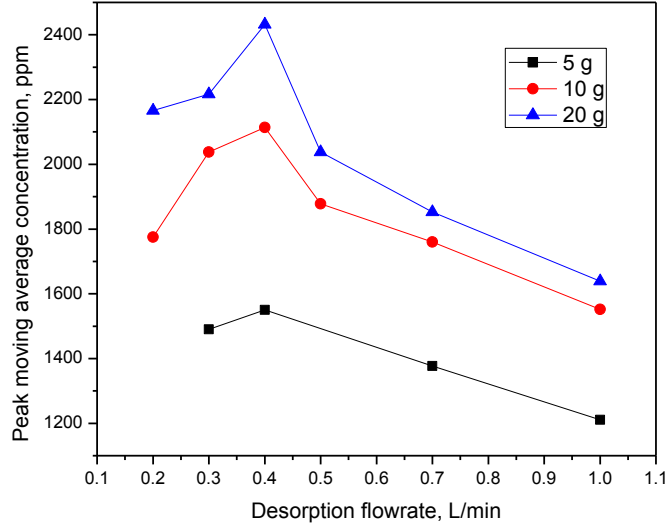


Figure 4-4 Peak moving average CO₂ concentration as a function of desorption flow rate.

4.2 Experiments with 1000 ppm CO₂

Although the target of this project is to enrich CO₂ from atmospheric level, which is about 400 ppm, experiments were carried out at two CO₂ concentrations, 1000 ppm and 400 ppm, in the current study to reveal the effect of CO₂ concentration on CO₂ enrichment. In this section, we report the experimental results obtained using 1000 ppm CO₂ on zeolite 13X at different adsorption and desorption temperatures.

4.2.1 Experimental conditions

20 g of 13X was loaded in the unit. According to the results of preliminary experiments, desorption flow rate was set at 0.4 L/min and an adsorption flow rate of 1 L/min was used. Experiments were conducted at four adsorption and desorption temperature differences (ΔT) of 20 °C, 15 °C, 10 °C and 5 °C, respectively.

4.2.2 Results and discussions

Adsorption and desorption capacities were calculated based on Equations (3-1) and (3-2), and the peak moving average concentration ($c(\text{ave})_{\text{max}}$) was obtained and summarized in Table 4-1.

Table 4-1 Adsorption capacity, desorption capacity and peak concentration (1000 ppm CO₂)

	$T_{\text{ad}}, ^\circ\text{C}$	$T_{\text{de}}, ^\circ\text{C}$	$q_{\text{ad}}, \text{mol/kg}$	$q_{\text{de}}, \text{mol/kg}$	$c(\text{ave})_{\text{max}}, \text{ppm}$	$q_{\text{de}}/q_{\text{ad}}$
$\Delta T=20 ^\circ\text{C}$	5	25	0.0489	0.0328	2666	0.67
	10	30	0.0395	0.0276	2272	0.70
	20	40	0.0356	0.0221	2121	0.62
	30	50	0.0259	0.0203	1990	0.78
$\Delta T=15 ^\circ\text{C}$	10	25	0.0403	0.0244	2062	0.60
	20	35	0.0321	0.0154	1831	0.48
	30	45	0.0264	0.0044	1745	0.17
$\Delta T=10 ^\circ\text{C}$	5	15	0.0488	0.0155	1874	0.32
	10	20	0.0422	0.0142	1472	0.33
	15	25	0.0330	0.0139	1577	0.42
	20	30	0.0304	0.00743	1435	0.24
	25	35	0.0289	0.00521	1430	0.18

$\Delta T=5\text{ }^{\circ}\text{C}$	5	10	0.0421	0.00542	1189	0.13
	15	20	0.0362	0.00306	1150	0.084

Figure 4-5, Figure 4-6, Figure 4-7 and Figure 4-8 show the enrichment factor curves as a function of desorption time. After about 10 minutes of desorption, the enrichment factor reaches a peak and then drops gradually.

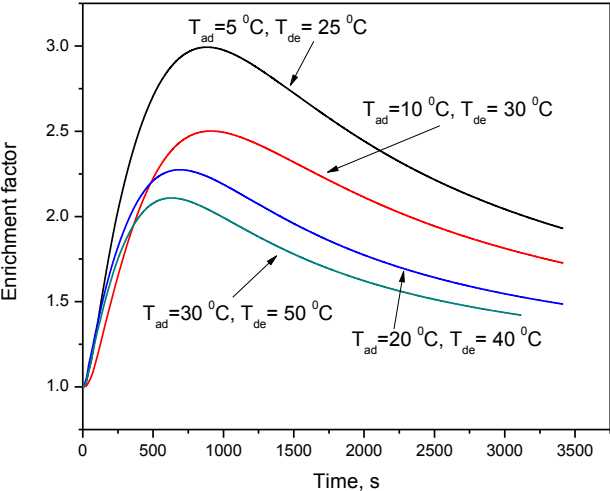


Figure 4-5 Enrichment factor as a function of desorption time (1000 ppm CO₂, $\Delta T=20\text{ }^{\circ}\text{C}$)

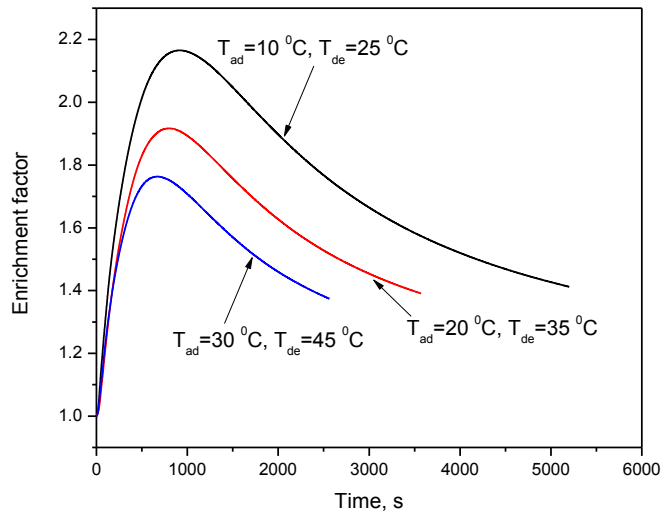


Figure 4-6 Enrichment factor as a function of desorption time (1000 ppm CO₂, ΔT=15 °C)

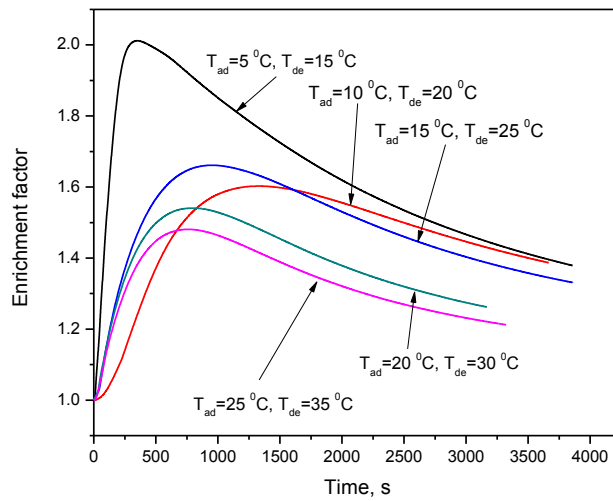


Figure 4-7 Enrichment factor as a function of desorption time (1000 ppm CO₂, ΔT=10 °C)

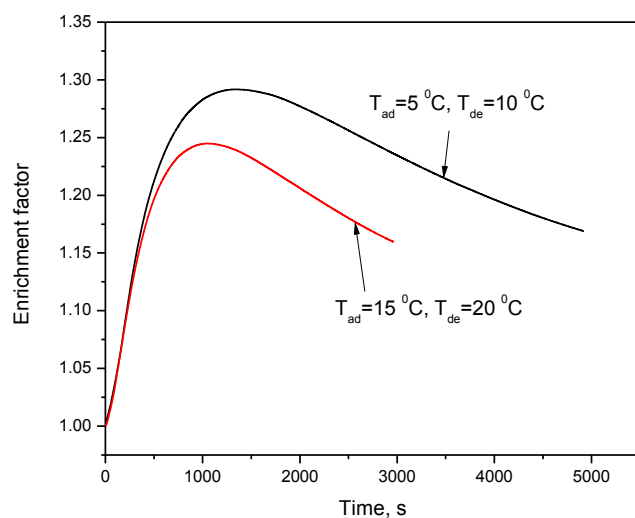


Figure 4-8 Enrichment factor as a function of desorption time (1000 ppm CO₂, $\Delta T=5$ °C)

In order to show how temperature affects the adsorption and desorption performances, the adsorption and desorption capacities of different experimental conditions were obtained and plotted in Figure 4-9 and Figure 4-10.

Figure 4-9 shows the adsorption capacity at four different temperature differences of 20 °C, 15 °C, 10 °C and 5 °C. It is seen that adsorption capacity is a strong function of adsorption temperature, decreasing with increasing the adsorption temperature. At the same adsorption temperature, the adsorption capacity remained almost the same, independent of desorption temperature.

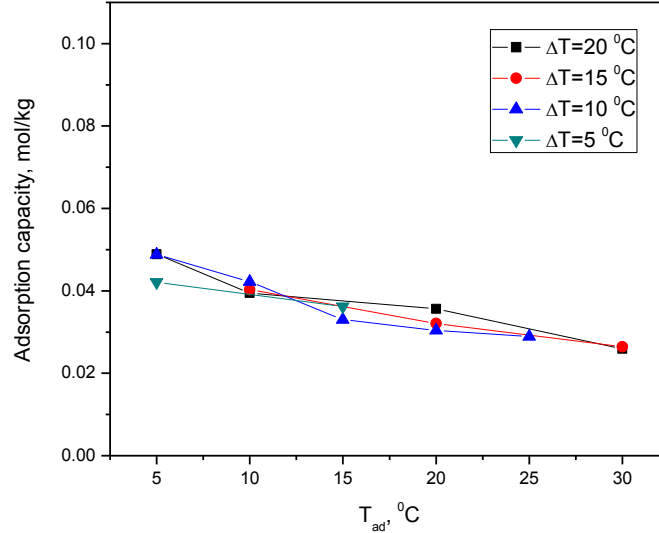


Figure 4-9 Adsorption capacity versus adsorption temperature at four different adsorption-desorption temperature differences (1000 ppm CO₂)

Figure 4-10 shows the desorption capacity as a function of desorption temperature. Four curves represent the results obtained at four adsorption temperatures of 5 °C, 10 °C, 20 °C and 30 °C. Different from the adsorption capacity curves, desorption capacity depends not only on the adsorption temperature but also the desorption temperature. For each curve at a same adsorption temperature, desorption capacity increases as desorption temperature increases, as expected. At a constant desorption temperature, it is seen that the desorption capacity decreases as adsorption temperature is increased because the increase in the adsorption temperature lowered the adsorption capacity. Because of less CO₂ being adsorbed in the adsorbent, less CO₂ is desorbed during desorption period.

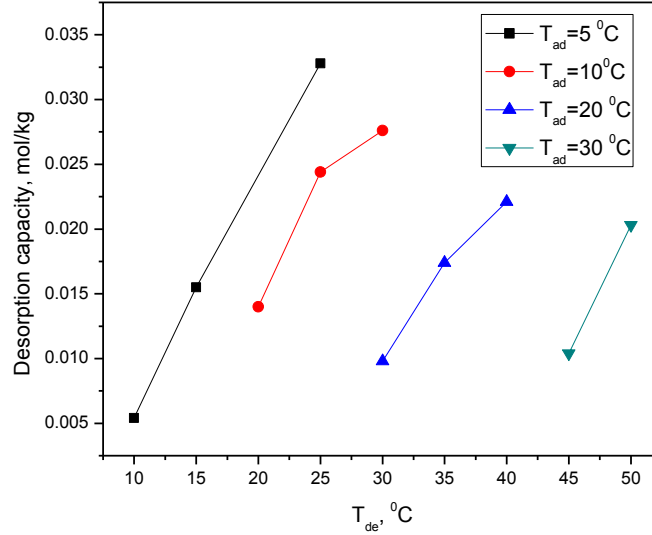


Figure 4-10 Desorption capacity as a function of desorption temperature (1000 ppm CO₂)

Figure 4-11 shows the relationship between maximum enrichment factor and adsorption temperature. The factor is seen to be higher at larger temperature differences. The results suggest that one should operate the unit at a low adsorption temperature and high desorption temperature, or at a large temperature difference, in order to achieve a higher CO₂ concentration in the enriched gas stream.

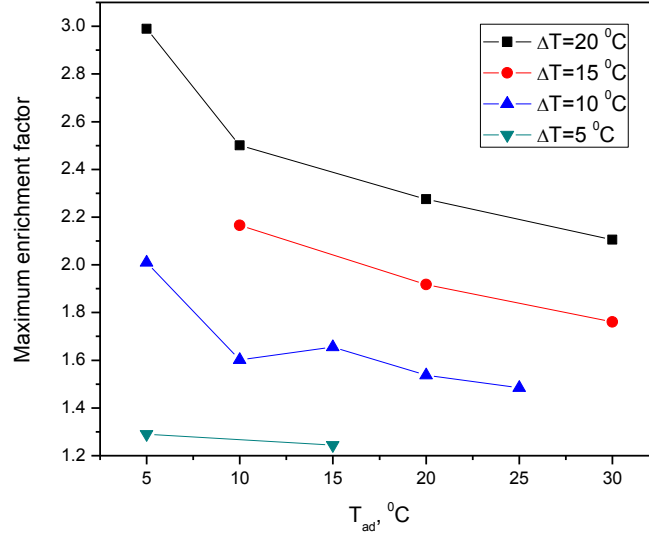


Figure 4-11 Maximum enrichment factor at different adsorption temperatures (1000 ppm)

4.3 Experiments with 400 ppm CO₂

The performance of 20 g zeolite 13X at different adsorption and desorption temperatures were tested in order to assess the possibility of enriching CO₂ concentration from 400 ppm to 1000 ppm.

4.3.1 Experimental conditions

The same as in the previous experiment, 20 g of 13X was first loaded into the unit. Desorption flow rate was then selected as 0.4 L/min and the adsorption flow rate was selected as 1 L/min. A total of three sets of experiments were conducted at adsorption and desorption temperature differences of 20 °C, 15 °C and 10 °C, respectively.

4.3.2 Results and discussions

Adsorption capacity and desorption capacity were calculated following the same procedures as described before, and the peak concentration for each test was obtained and summarized in Table 4-2.

Table 4-2 Adsorption capacity, desorption capacity and peak concentration (400 ppm CO₂)

	$T_{ad}, ^\circ C$	$T_{de}, ^\circ C$	$q_{ad}, mol/kg$	$q_{de}, mol/kg$	$c(ave)_{max}, ppm$	q_{de}/q_{ad}
$\Delta T=20 ^\circ C$	10	30	0.0262	0.0189	1133	0.72
	20	40	0.0242	0.0142	1081	0.59
	30	50	0.0207	0.00841	881	0.41
$\Delta T=15 ^\circ C$	10	25	0.0321	0.0143	849	0.44
	15	30	0.0271	0.0118	832	0.43
	20	35	0.0223	0.0122	806	0.55
$\Delta T=10 ^\circ C$	10	20	0.0291	0.00625	615	0.21
	20	30	0.0245	0.00354	588	0.14

Figure 4-12, Figure 4-13 and Figure 4-14 present the enrichment factor curves at different test conditions. After about 10 minutes of desorption, the enrichment factor reaches a peak and then decreases gradually.

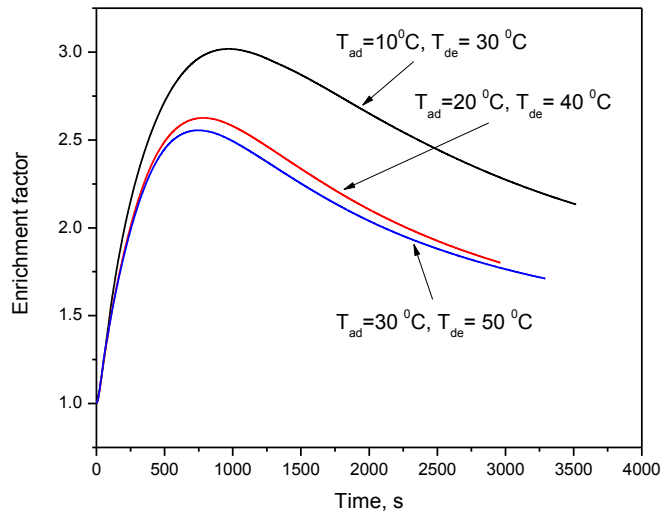


Figure 4-12 Enrichment factor as a function of desorption time (400 ppm CO₂, ΔT=20 °C)

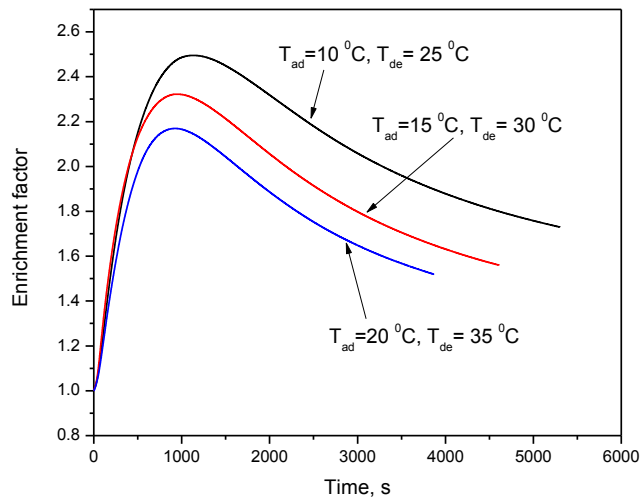


Figure 4-13 Enrichment factor as a function of desorption time (400 ppm CO₂, ΔT=15 °C)

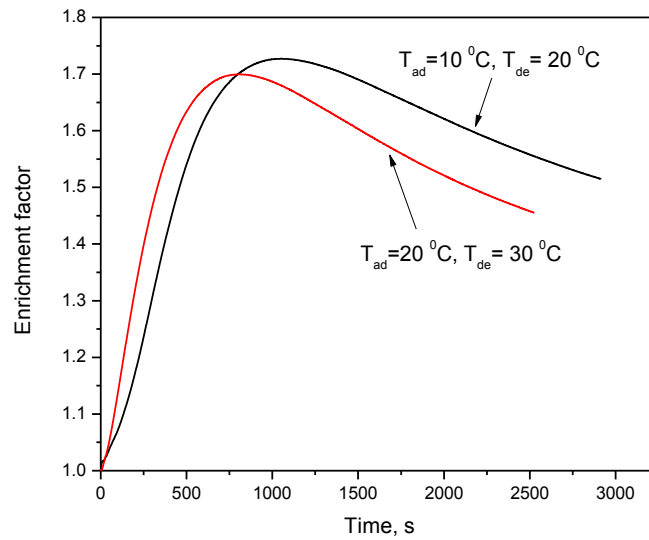


Figure 4-14 Enrichment factor as a function of desorption time (400 ppm CO₂, ΔT=10 °C)

It is clearly seen from Figure 4-15 that the adsorbent has almost the same adsorption capacity at the same adsorption temperature. The desorption capacity as a function of desorption temperature was plotted in Figure 4-16. The same conclusion as drawn from Figure 4-10 can be reached that both adsorption temperature and desorption temperature will have an influence on desorption capacity. When adsorption temperature is kept the same, desorption capacity will increase as desorption temperature increases. If desorption takes place at the same temperature, desorption capacity will increase along with the decrease of adsorption temperature.

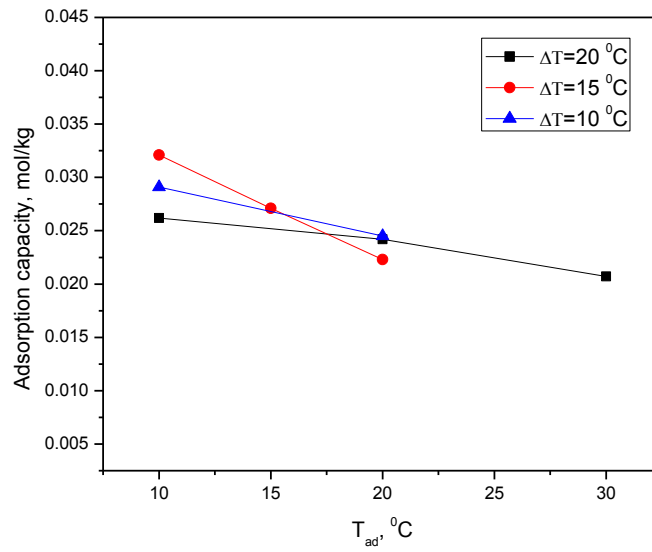


Figure 4-15 Adsorption capacity versus adsorption temperature at four different adsorption-desorption temperature differences (400 ppm)

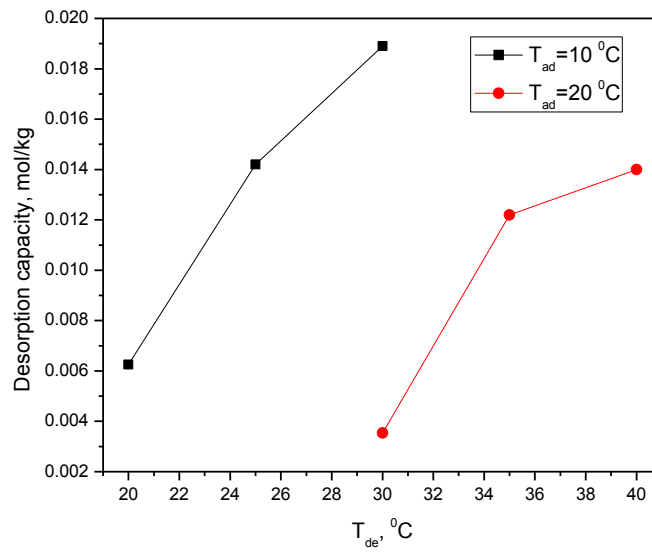


Figure 4-16 Desorption capacity as a function of desorption temperature (400 ppm)

Figure 4-17 shows the maximum enrichment factors at different adsorption and desorption temperatures. Similar to the results shown in Figure 4-11 for 1000 ppm CO₂, the lower adsorption temperature and higher desorption temperature give rise to a higher enrichment factor, because of a higher adsorption capacity and faster desorption rate.

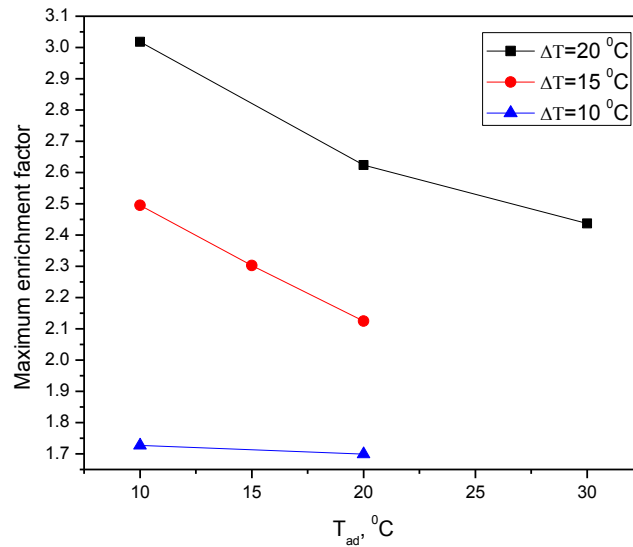


Figure 4-17 Maximum enrichment factor at different adsorption temperatures (400 ppm)

Since the focus of the current project is to investigate the feasibility of enriching CO₂ from 400 ppm to about 1000 ppm for stimulating crop growth in greenhouses, data in Figure 4-17 show that a maximum enrichment factor of 3 can be reached, making it feasible to enrich the ambient air CO₂ concentration from 400 ppm to 1200 ppm.

4.3.3 Experimental error analyses

In order to make an analysis on the experimental errors, some experiments were repeated with gas at 400 ppm CO₂. Experimental conditions and results are listed in Table 4-3.

Table 4-3 Error analyses for several repeated experiments with 400 ppm CO₂

(a) Adsorption capacity

Experimental conditions	Adsorption capacity, mol/kg				Relative error, %		
	T _{ad} , °C	1	2	3	Average	1	2
20	0.0242	0.0226	0.0245	0.0238	1.8	4.9	3.1
15	0.0271	0.0263	0.0274	0.0269	0.6	2.3	1.7
10	0.0291	0.0262	0.0321	0.0291	10.0	0.11	10.1

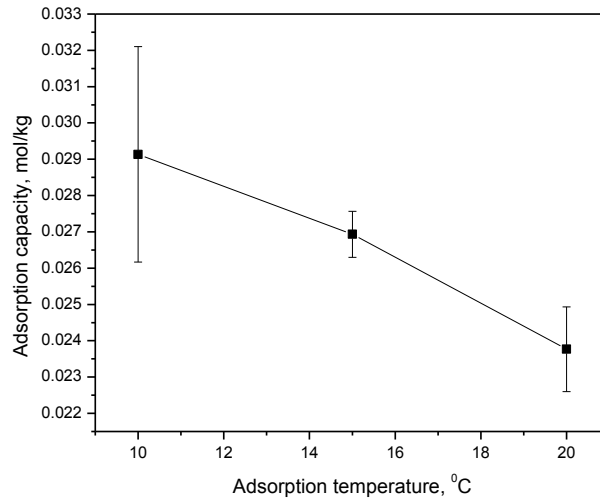
(b) Desorption capacity

Experimental conditions		Desorption capacity, mol/kg			Relative error, %
T _{ad} , °C	T _{de} , °C	1	2	Average	
20	40	0.0142	0.0154	0.0148	4.1
15	30	0.0118	0.0114	0.0116	1.7
10	20	0.00625	0.00809	0.007145	13.2

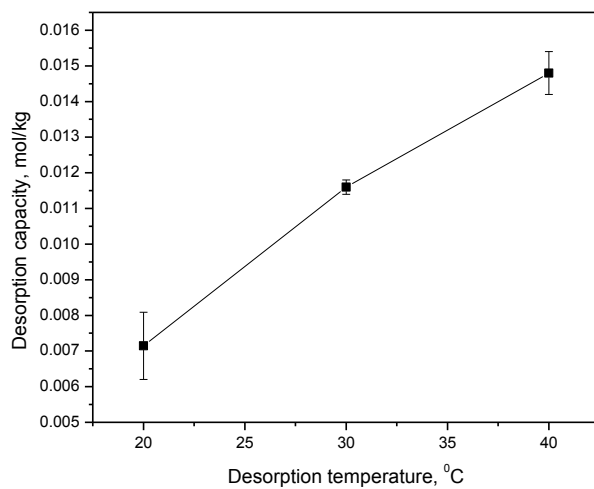
(c) Peak moving average concentration

Experimental conditions		Maximum moving average concentration, ppm			Relative error, %
T _{ad} , °C	T _{de} , °C	1	2	Average	
20	40	1081	1184	1132.5	4.5
15	30	832	811	821.5	1.3
10	20	615	768	691.5	11.1

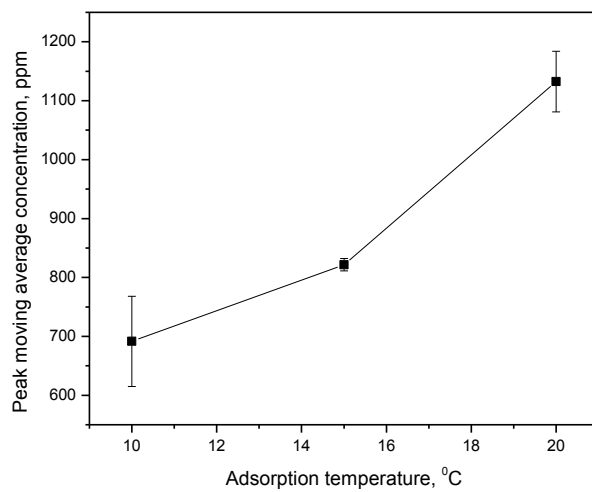
The relative errors of adsorption capacity, desorption capacity and peak moving average concentration were calculated, which were in a range less than 13%. The error bars for each experiment were plotted in Figure 4-18.



(a) Adsorption capacity



(b) Desorption capacity



(c) Peak moving average concentration

Figure 4-18 Average adsorption capacity, desorption capacity and peak moving average concentration with error bars included

4.3.4 Correlations for adsorption capacity

Several adsorption models, including Langmuir equation, Freundlich equation and BET equation, can be used to correlate the adsorption capacity with concentrations of CO₂ at different temperatures. To select a suitable model, more experiments were conducted with a CO₂ concentration of 500 ppm, 600 ppm, 700 ppm, 800 ppm and 900 ppm, at an adsorbent loading of 20 g, adsorption temperature of 10 °C and desorption temperature of 30 °C.

Based on the experimental results, we found that the data were best fitted to the Freundlich model equation (Equation 4-2 below), as shown in Figure 4-19.

$$q = kp^{\frac{1}{n}} \quad (4-2)$$

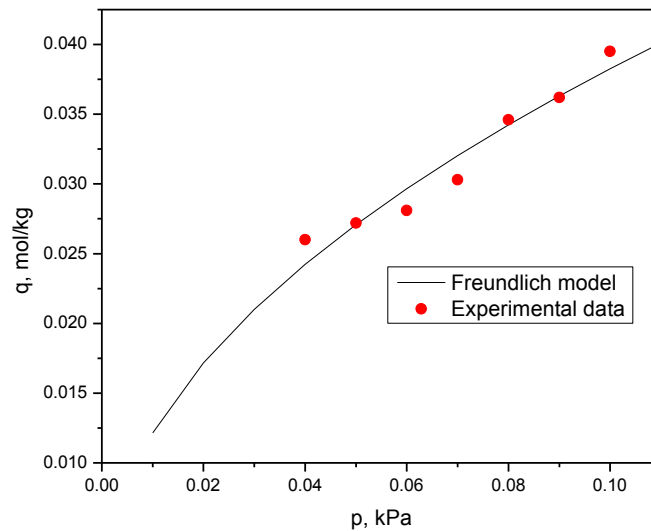


Figure 4-19 Data fitting to Freundlich model equation

The model parameters, k and n , are dependent on adsorption temperature and were obtained by fitting the Freundlich equation to data at different temperatures.

$$n = 0.0744T - 18.685 \quad (4-3)$$

$$k = 2.16 \times 10^{-7} \times \exp\left(\frac{3713}{T}\right) \quad (4-4)$$

4.4 Moisture effects

All the experiments shown above were performed under dry conditions. The performance of adsorbents might be influenced by the presence of moisture in atmospheric air. Therefore, experiments were conducted to investigate the moisture effect on the adsorption and desorption of low concentration CO₂ on zeolite 13X.

4.4.1 Experimental setup

The whole process, as shown in Figure 4-20, was kept the same as in the previous study, and the only difference was the addition of a humidification unit as shown in Figure 4-21. Before the dry gas stream enters the column, the gas flow is split with one stream passing through a humidifier to pick up moisture. The flow rate of the gas stream passing through the humidifier was controlled by a needle valve, resulting in various relative humidity (RH) of the combined gas stream entering the adsorption column. The performance was evaluated at different RH conditions at given adsorption and desorption temperatures.

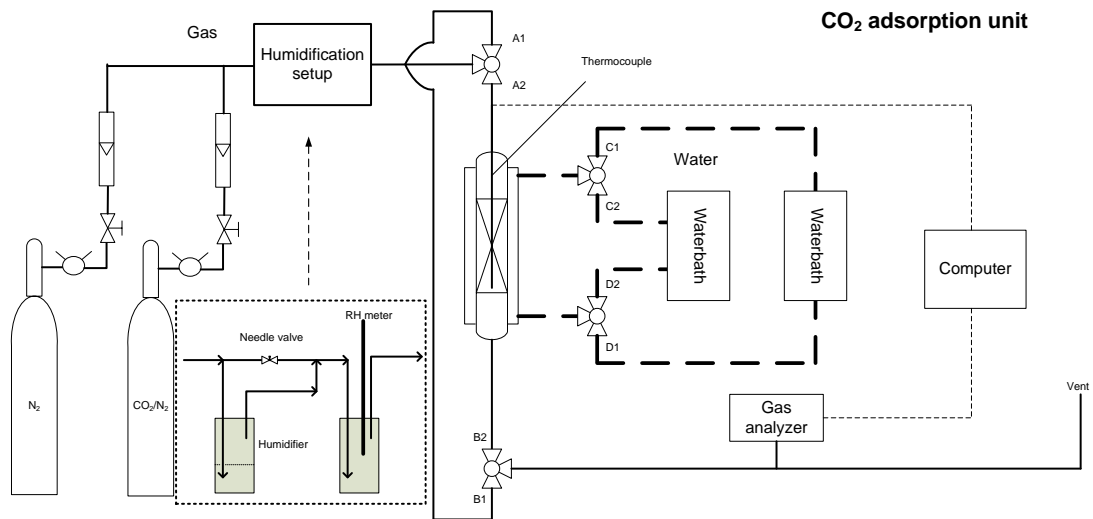


Figure 4-20 Process diagram of CO₂ adsorption and desorption unit with humidification setup



Figure 4-21 Humidifier setup

20 g of 13X was used in the experiment. The same as in previous experiments, desorption flow rate was set at 0.4 L/min, and the adsorption flow rate at 1 L/min. Three sets of experiments were conducted. For each set of experiments, the only variable was relative humidity, varied from 0 to 80 %, while the adsorption and desorption temperatures were kept at constant. The adsorption/desorption temperatures in each set of tests were 5 °C/25 °C, 5 °C/30 °C and 10 °C/30 °C, respectively.

4.4.2 Results and discussions

The adsorption capacity, desorption capacity and maximum moving average concentration were calculated using equations (3-1) and (3-2) and shown below.

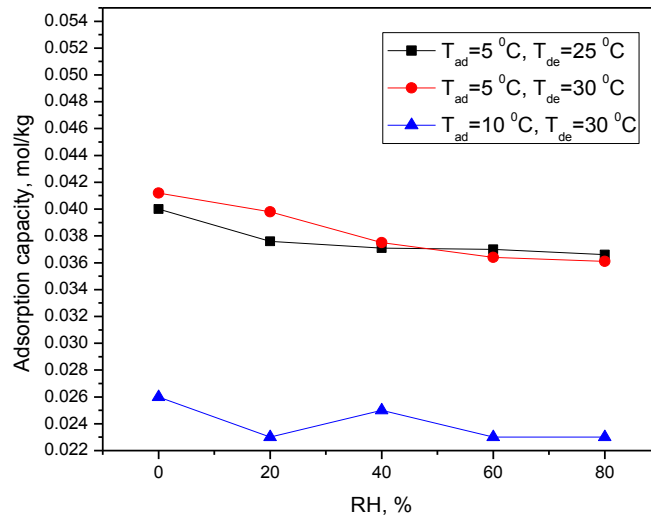


Figure 4-22 Adsorption capacities at different RH

In Figure 4-22, the adsorption capacity of 13X at 5 °C were 0.0402, 0.0376, 0.0371, 0.037 and 0.0366 mol/kg at a RH of 0, 20%, 40%, 60% and 80 %, respectively, while desorption

temperature was 25 °C. The capacity in moisture air was about 8.5% lower than that in dry condition. There was little variation at different relative humidities. The adsorption capacity of 13X at 10 °C were 0.0262, 0.0232, 0.0251, 0.0233, and 0.0232 mol/kg at RHs of 0, 20, 40, 60 and 80 %, respectively, at a desorption temperature of 30 °C. The capacity showed an 11.5% decrease as the RH increased from 0 to 20%. With further increase in RH, no noticeable decrease in capacity was observed. It was also reported by Su[81] that a decrease of 25% and 11.5% in adsorption capacity was observed with a rise in RH from 0 to 99% at 40 °C and 30 °C, respectively. They concluded that 13X displayed an acceptable moisture sensitivity and possessed a stable adsorption performance for CO₂ under humid conditions below 30 °C.

The desorption capacities with humidified gases were shown in Figure 4-23. Unlike the adsorption capacity data in Figure 4-22, a sharp decrease in desorption capacity was observed at low RH. When desorption took place at 30 °C, desorption capacity showed a decrease of 21.5% ($T_{ad}=10$ °C) and 31.6% ($T_{ad}=5$ °C) as RH increased from 0 to 20%. However, at a desorption temperature of 25 °C, the decrease was only 10.7%. These sharp decreases in desorption capacity at 30 °C indicate that the adsorbent tends to be sensitive to moisture at 30 °C. This could be explained by blockage of diffusion channels by the adsorbed water vapour during the CO₂ desorption at higher desorption temperatures. At temperatures lower than 25 °C, 13X showed stable CO₂ adsorption performance under humid conditions.

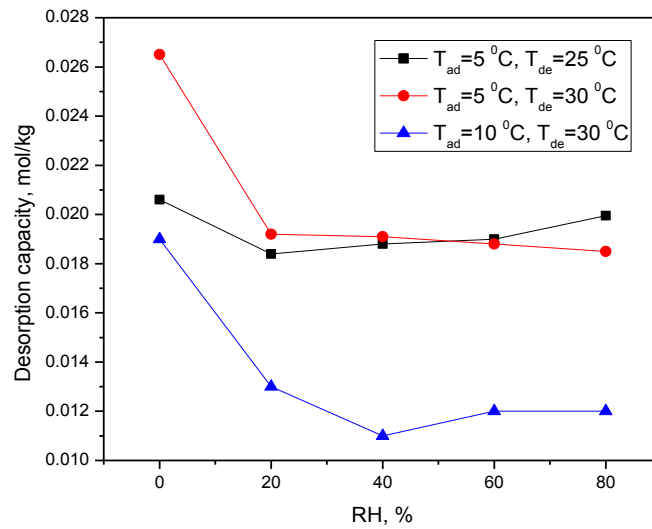


Figure 4-23 Desorption capacities at different RH

Besides the adsorption/desorption capacities, the maximum moving average concentration is also an important factor for consideration. The results in Table 4-4 showed that when the temperature difference was set at 25 °C, it was impossible to reach the target of 1000 ppm CO₂. A further increase of ΔT to 30 °C would give rise to a peak moving average CO₂ concentration above 1000 ppm.

Table 4-4 Peak moving average concentrations with a RH of 20% at different temperatures

T_{ad} , °C	T_{de} , °C	RH, %	$c(ave)_{max}$, ppm
10	30	20	794
5	25	20	864
5	30	20	1060
5	35	20	1260

4.5 Summary

In summary, 13X has proved to perform well in the CO₂ adsorption and desorption at low concentrations similar to that in the ambient air. The adsorption capacity was 0.026 mol/kg at 10 °C and the desorption capacity was 0.0189 mol/kg at 30 °C. A maximum enrichment factor of 3 from the experiment indicated the feasibility of CO₂ enrichment from 400 ppm to 1000 ppm. In spite of the fact that moisture has an effect on the performance of 13X above 25 °C, the target level of 1000 ppm can still be reached by increasing the adsorption and desorption temperature difference to above 30 °C. In the actual design and operation of such a CO₂ enrichment system, it is thus recommended to keep an adsorption and desorption temperature difference above 30 °C, while maintaining the adsorption temperature as low as possible.

Chapter 5 Economics analyses

5.1 Cost analyses of CO₂ enrichment by TSA directly from air

The total cost includes capital cost and operating cost. Capital cost for this project is associated with the purchase of adsorbents and the equipment, while the operating cost is mainly related to the cost of energy needed for temperature swing adsorption and equipment maintenance.

5.1.1 Capital cost

It is quite straightforward to estimate the capital cost for the packed bed column, which includes purchased cost of adsorbent and the unit, cost of auxiliary equipment and building, and installation cost.

Due to the low temperature operation, the adsorbent can be regenerated over an extended period of many years. When calculating the capital cost, it is necessary to annualize the cost based on the annual interest rate. The adsorbent we have tested is 13X zeolite. The unit price of 13X zeolite is about \$2000 per metric tonne (T), and the lifetime of the whole unit is assumed to be 15 years. The annual interest rate is set at 10%, compounded annually. Annualized capital cost can be calculated based on the following equation:

$$C_{cap} = PV * (1 + i)^m * i / [(1 + i)^m - 1] \quad (5-1)$$

where PV represents the present value of total capital cost, i is the effective annual interest rate, and m is the life time of the equipment in number of years.

5.1.2 Operating cost

Operating cost mainly refers to the cost needed to run the unit, which is the consumed energy, and the maintenance cost.

During the operation of the whole process, an air blower is needed to pass the air through the unit. In this case, electricity is needed. For temperature swing adsorption, additional heating is required to raise the air temperature to the level desired for desorption. Greenhouses commonly require heat to maintain a certain temperature suitable for plant growth, so the heat from burning natural gas or geothermal will be used to offset the heat requirement of the greenhouse. Therefore, the cost for heating in the desorption stage will be excluded in the operating cost in the current analysis.

The air blower needs power to overcome the pressure drop across the fixed sorbent bed. So the pressure drop of the fixed bed was calculated to estimate the required electrical energy. On the laboratory scale unit, 20 g of 13X was loaded in the fixed bed at a gas flow rate of 1 L/min. In a commercial scale, more than 10 tonnes (T) sorbents will be used. To maintain the same space velocity, the gas flow rate in the industrial scale can be calculated as,

$$Q = \frac{M}{M_{exp}} Q_{exp} \quad (5-2)$$

where M is the adsorbent loading in the industrial unit, M_{exp} and Q_{exp} are adsorbent loading and gas flow rate in the laboratory unit, respectively. Superficial gas velocity and specific surface area can be obtained by the following equations,

$$u = \frac{Q}{A} = \frac{Q}{\frac{1}{4}\pi D^2} \quad (5-3)$$

$$a = \frac{S}{V} = \frac{4\pi\left(\frac{d_p}{2}\right)^2}{\frac{4}{3}\pi\left(\frac{d_p}{2}\right)^3} = \frac{6}{d_p} \quad (5-4)$$

where d_p is the average particle diameter of spherical adsorbent particles. Ergun equation is applied here to estimate the pressure drop across the fixed bed.

$$\frac{\Delta P}{L} = 4.17 \frac{(1 - \varepsilon)^2 a^2}{\varepsilon^3} \mu u + 0.29 \frac{(1 - \varepsilon) a}{\varepsilon^3} \rho u^2 \quad (5-5)$$

Finally, the electricity consumption for the operation of air blower is

$$E_{elec} = \Delta P * \left(\frac{1}{4} \pi D^2\right) * L / \eta \quad (5-6)$$

where η is the energy efficiency of air blower. The cost of electricity can be estimated by

$$C_{elec} = E_{elec} * \text{Electricity unit price} \quad (5-7)$$

5.1.3 Unit price of CO₂

It takes about three hours to complete one cycle of temperature swing adsorption and desorption. Since there is no need for CO₂ during the night when there is no photosynthesis, we can assume that the unit can be operated 12 hours a day. Thus in a single day, 3 to 4 cycles can be carried out to increase the amount of CO₂ captured. The unit price of CO₂ desorbed can be estimated by

$$Unit\ price = \frac{Total\ cost}{Amount\ of\ CO_2\ desorbed} = \frac{Capital\ cost + Operating\ cost}{Amount\ of\ CO_2\ desorbed} = \frac{C_{cap} + C_{elec} \times p}{M \times q_{de} \times p} \quad (5-8)$$

where p is the number of daily operation cycles.

Figure 5-1 shows the purchased equipment costs for the adsorption/desorption vessel with different volumes. An average annual rate of inflation of 1.83% according to the data from Bank of Canada was used for adjustment in equipment price in following calculations. In this case, the vessel material is carbon steel. Table 5-1 shows the cost of the unit as well as annualized capital costs at different adsorbent loadings.

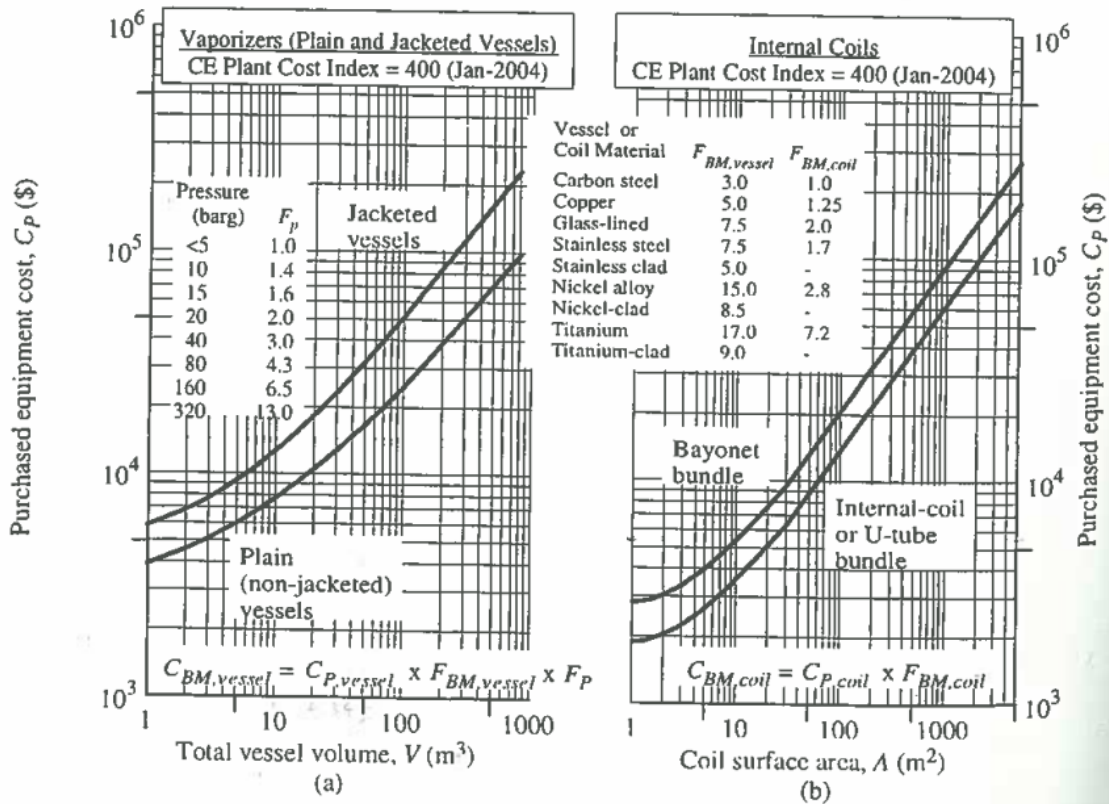


Figure 5-1 Purchased equipment cost[85]

Table 5-1 Capital costs at different adsorbent loadings

Adsorbent loading, T	10	15	20	25
Cost of adsorbents, \$	20,000	30,000	40,000	50,000
Dimensions of the vessel (D×L), m×m	2.5×4.2	3.0×4.3	3.5×4.2	3.5×5.3
Cost of the vessel, \$	35,971	39,568	50,359	57,554
Cost of auxiliary equipment and building, \$	3,597	3,957	5,036	5,755
Installation cost, \$	1,798	1,978	2,518	2,878
Annualized capital cost, \$	8,068	9,927	12,873	15,275

Main assumptions used in the calculation are listed in Table 5-2. Using the equations and assumptions presented above, CO₂ unit prices under different circumstances are calculated and presented in Figure 5-2.

Table 5-2 Main assumptions used in the calculation

Items	Assumptions
Annual interest rate	10% (compounded annually)
Lifetime of the equipment and the adsorbent	15 years
Vessel material	Carbon steel
Adsorption temperature	Ambient temperature
Electrical efficiency of air blower	80%
Duration for each adsorption and desorption cycle	3 hours
Number of daily operation cycles	4
Installation cost	5% of the equipment cost[85]
Maintenance cost	3% of the equipment cost[85]
Cost of auxiliary equipment and building	10% of the equipment cost[85]
Other assumptions:	
The adsorption and desorption capacity is kept the same in all cycles;	
Other costs that are not given here are negligible.	

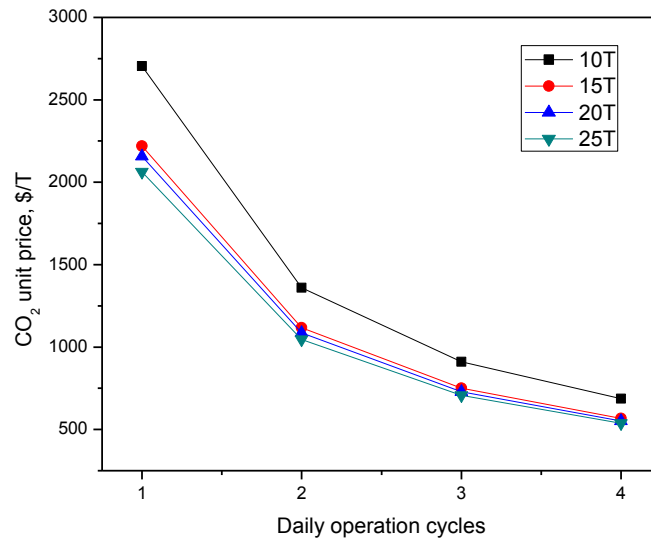


Figure 5-2 CO₂ unit price as a function of daily operation cycles at different adsorbent loadings

As the daily adsorption and desorption cycles increase, the unit price decreases significantly. The adsorbent loading also has an influence on the unit price. When adsorbent loading changes from 10 T to 15 T, the CO₂ unit price is reduced clearly. However further increasing adsorbent loading to 20 T, the unit price is reduced only marginally from \$567/T to \$551/T if four cycles are run per day. The reduction is non-significant compared with the reduction from 10 T to 15 T. This is mainly due to the increased equipment cost. Compared with the enhanced adsorption and desorption performance while increasing the adsorbent loading, the total price seems to be dominated by the increase in equipment cost. In the current analyses, an adsorbent loading of 15 T is selected for further analyses. The CO₂ unit price is estimate to be \$567/T with a sorbent loading of 15 T and 4 adsorption and desorption cycles running per day.

5.1.4 Sensitivity analysis of CO₂ unit price to the adsorbent performance

According to the results in Figure 5-2, the lowest CO₂ unit price by temperature swing

adsorption directly from ambient air is predicted to be \$538/T-CO₂ based on the adsorption/desorption performance data obtained in the current experimental results using the tested 13X adsorbent. Such a high cost may result from the too low adsorption capacity of the tested adsorbent, as the CO₂ adsorption capacity as high as 10 times what we obtained has been reported in the literature [36, 47, 65, 82]. The desorption capacity of 13X at 30 °C obtained from the current experiments was 0.019 mol/kg. It was reported by Wang [83] that the 13X zeolite tested in their study had an adsorption capacity of 0.178 mol /kg at 60 °C. By assuming a same desorption to adsorption ratio based on our experimental data, the desorption capacity of 13X from Wang [12] is 0.129 mol/kg, 6.7 times the capacity from the current experiment.

A sensitivity analysis with respect to the desorption capacity is thus carried out to check the sensitivity of CO₂ unit price to the adsorption/desorption capacity. Table 5-3 shows the CO₂ unit price as the adsorption capacity is increased by twice, four times, six times, eight times and ten times. If the capacity was improved by six times, the unit price could potentially drop to as low as \$94/T-CO₂. Regardless of the adsorption capacity, capital cost is always the dominant contribution to the total cost. It should be noted that much higher adsorption capacities, >1 mol/kg, have been reported in the literature using advanced amine-supported adsorbents [67, 71, 73]. A unit price of CO₂ at \$15/T-CO₂ is thus expected to be a reasonably achievable target using the current proposed temperature swing adsorption technology to enrich CO₂ from air for greenhouse applications.

Table 5-3 Sensitivity analyses of CO₂ unit price to desorption capacity

Desorption capacity	Unit price	Capital cost	Operating cost
mol/kg	\$/T-CO₂	\$/T-CO₂	\$/T-CO₂
0.019 (current study)	567	542	25
0.019×2	284	271	13
0.019×4	142	135	7
0.019×6	94	90	4
0.019×8	71	68	3
0.019×10	57	54	3

The adsorbent of 13X was purchased at a cost of \$2000/T, and other adsorbents with high adsorption capacity may also be more expensive. Therefore, an analysis on the sensitivity of CO₂ unit price to the adsorbent costs is also conducted to examine the combined impact of adsorbent price and adsorption capacity on the CO₂ unit cost. Figure 5-3 shows the CO₂ unit price as a function of adsorption capacities, ranging from 0.02 mol/kg to 2 mol/kg at four adsorbent costs of \$2,000/T, \$5,000/T, \$10,000/T and \$20,000/T. The results show that the adsorption capacity has more significant effect on the CO₂ unit price than the adsorbent price. When adsorption capacity increased from 0.02 mol/kg to 0.4 mol/kg, the unit cost significantly decreased by 95% at all four adsorbent costs. There is no noticeable reduction in unit cost when the adsorption capacity is further increased. It indicates that in order to get a low CO₂ unit price by proposed method, the crucial factor is the adsorption capacity no matter how high the adsorbent cost is.

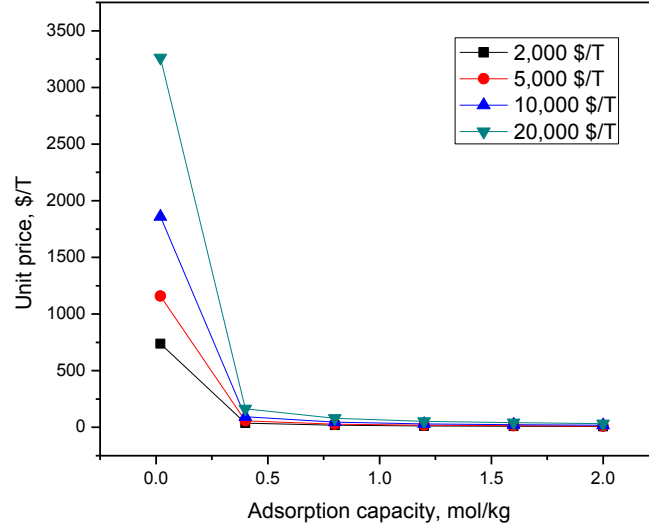


Figure 5-3 Sensitivity analyses of unit price to adsorbent price and adsorption capacity

5.2 Costs for different scenarios to provide heat and CO₂ to greenhouses

In a greenhouse, large amount of heat and certain amount of CO₂ are essential for the growth of crops. The heating requirement in a typical greenhouse is estimated at 2.25 GJ/m².yr, and CO₂ requirement is 75 kg/m².yr[86]. They may come from various sources. Traditionally, both heat and CO₂ demands in the greenhouse have been provided by burning natural gas. Some greenhouses operating with renewable energy sources, e.g. biomass, geothermal, solar and waste heat, obtained CO₂ from other sources.

By burning natural gas, it provides both heat and relatively clean CO₂ as well. When heat is not needed in summer days, hot water is used to store heat for use at night with most heat being wasted. When heat is provided from renewable energy sources, including solar energy,

geothermal energy or burning biomass or municipal wastes, CO₂ in greenhouses can be supplied from burning natural gas as well as from purchasing pure liquefied CO₂. Alternatively, as proposed in this work, CO₂ enrichment can be provided by temperature swing adsorption on adsorbents. As for industrial applications, it is suggested that a dual bed system can be applied. When one bed is at adsorption period, the other one will work at desorption stage with enriched CO₂ gas stream flowing to greenhouses, providing steady flow of enriched CO₂ gas stream to greenhouses to maintain a stable CO₂ concentration in the greenhouse. Different scenarios to provide heat and CO₂ to greenhouses are listed in Table 5-4.

Table 5-4 Different scenarios to provide heat and CO₂ to greenhouses

	Heat source	CO₂ supply
	1 Natural gas combustion	Natural gas combustion
	Biomass combustion	Liquefied CO ₂
Scenarios	2 Solar or geothermal	CO ₂ enrichment by TSA with adsorbent
	Waste heat from nearby incineration or power plants	

The cost for each method is discussed and compared. Natural gas combustion can produce large amount of CO₂, with a combustion energy efficiency of >80%. Although there's a chance to produce CO and VOCs as well, in properly designed and controlled boilers, nearly all of the carbon in natural gas is converted to CO₂ in high efficiency combustors. To produce 1 kg of CO₂, the amount of natural gas needed is $\frac{16}{44} kg$. The unit price is calculated to be \$149 /T for a natural

gas price of \$8.8/GJ. Heat is also generated by natural gas combustion. Therefore the total fuel cost of \$149/T includes the supply of CO₂ and heat for the greenhouse. Based on the heat and CO₂ demands ratio in greenhouses of 56:191[87], the unit price for CO₂ can be estimated to be \$115/T-CO₂.

For the purchased pure CO₂, food grade CO₂ in tanks is available from gas companies such as Praxair at a price of about \$170/T. Unlike burning natural gas or purchasing pure CO₂, CO₂ enrichment by temperature swing adsorption directly capture CO₂ from the air creating a CO₂ credit as well.

5.3 Costs for using other methods to capture CO₂ directly from air

Most of the air CO₂ capture processes proposed in the literature are based on chemical absorption using alkaline solutions. Keith[29] proposed a processes using sodium hydroxide, followed by the causticization with lime and calcination. The cost for this process was estimated to be \$136 /T-CO₂. Nikulshina[88] developed an aerosol-type carbonator for capturing CO₂ from air using a spray tower with Ca(OH)₂ aqueous solution. The reported cost was amount to \$160-200 /T-CO₂. Stolaroff [89] proposed a method to capture CO₂ from ambient air using NaOH solution. . A model system using a NaOH spray tower was presented, with the cost for capturing CO₂ from air being estimated to be around \$130 /T-CO₂. Another approach based on a solid sorbent in the form of an anionic exchange resin by moisture swing adsorption was presented by Lackner[36], with an estimated cost of \$220 /T-CO₂. Table 5-5 summarizes the reported costs of several air CO₂ capture technologies. The unit cost of air CO₂ capture falls in the range of \$130-220/T-CO₂.

Table 5-5 Cost of CO₂ capture by different air capture technologies

Authors	Processes	Cost, \$/T-CO ₂
Keith[29]	NaOH scrubbing, causticization with lime, calcinations	136
Nikulshina[88]	Aerosol-type carbonator using Ca(OH) ₂ , solar calciner, conventional slaker	162-200
Stolaroff[31]	Prototype contactor with a NaOH spray tower	~130
Lackner[36]	Filter with anionic exchange resin, air exchange, steam flush, compression	220

5.4 Comparison of costs for CO₂-enrichment for greenhouses

As analyzed above, the costs for CO₂ enrichment in greenhouses range from \$115 to \$170 per tonne by burning natural gas or purchasing pure CO₂ tanks. Using the absorption or adsorption technologies proposed in the literature to capture CO₂ directly from air, the costs ranges from \$136 to \$220 per tonne. Therefore, the CO₂ captured from air using the CCS technologies will be unlikely competitive in supplying CO₂ to the greenhouses. The technology proposed in the current study, which enriches the CO₂ concentration in the air to 1000 ppm by temperature swing adsorption using adsorbents, will have a CO₂ cost of \$567 per tonne based on the 13X adsorbent evaluated in the current study with an adsorption capacity of 0.026 mol/kg. However, based on the CO₂ adsorption capacity of 13X adsorbent reported in the literature (0.178 mol/kg), the CO₂ cost is expected to be in the range of \$83 per tonne. Furthermore, if the amine-supported adsorbent currently under development is to be used with a reported adsorption capacity of 1 mol/kg, the CO₂ cost can be potentially reduced substantially to a level lower than \$15 per tonne

CO₂. Therefore, there is a great potential to deploy the proposed air CO₂ enrichment technology to supply CO₂ for plant growth stimulation in greenhouses in the future, which is especially of great benefits to those greenhouses using renewable energy sources (e.g. geothermal and solar) for heating.

5.5 Summary

- 1) Based on the performance data of 13X adsorbent tested in the current study, the unit price of CO₂ by temperature swing adsorption from ambient air is around \$538/T-CO₂.
- 2) If the desorption capacity is 6 times higher than the current capacity, as reported in the literature by other researchers, CO₂ unit price could be reduced to as low as \$94 /T-CO₂, which is much lower than all other methods with a cost ranging from \$115 to \$220 /T-CO₂.
- 3) A very low desorption capacity in this study results in a very high CO₂ unit cost. The most important issue to lower the total cost is thus to develop adsorbent of high adsorption and desorption capacities.

Chapter 6 Conclusions and future work

6.1 Conclusions

The objective of this study is to experimentally evaluate the performance of selected adsorbents for enriching ambient CO₂ concentration from 400 ppm to 1000 ppm by temperature swing adsorption, therefore proving the possibility of its application in greenhouses for crops growth. In this study, 13X zeolite was selected as the adsorbent for temperature swing adsorption directly from the air. The adsorption and desorption performance were evaluated in a fixed bed reactor, the effect of moisture was discussed, and finally an economic analyses on proposed method were conducted.

According to the experimental results, the adsorption capacity is a function of only adsorption temperature. It decreases as adsorption temperature is increased. At the same adsorption temperature, the capacity remained almost the same. As for the desorption temperature, it will be influenced by both adsorption and desorption temperature. At a same adsorption temperature, desorption capacity increases as desorption temperature increases. However at a constant desorption temperature, the desorption capacity decreases as adsorption temperature is increased. Maximum enrichment factor was also discussed, and it can be concluded that the lower adsorption temperature and higher desorption temperature give rise to a higher enrichment factor. Therefore, in order to obtain higher CO₂ concentration in the enriched gas stream, it's suggested to run at a low adsorption temperature and high desorption temperature. Results have shown that a enrichment factor of 3 can be achieved in the experiments with 400 ppm CO₂, indicating the feasibility of CO₂ enrichment in greenhouses by temperature swing adsorption directly from the air.

It was revealed that 13X showed stable adsorption performance of CO₂ under humid conditions at temperatures lower than 25 °C and tends to be a little sensitive to moisture at 30 °C. However

the target level of 1000 ppm can still be reached by increasing the adsorption and desorption temperature difference to above 30 °C.

Based on the performance data of 13X adsorbent evaluated in the current study, the unit price of CO₂ by the proposed method is estimated to be \$567/T-CO₂ if 15T of adsorbents are loaded. This unit cost is much higher than other technologies to capture CO₂ directly from air, which is mainly due to the obtained low adsorption and desorption capacity. If the capacity can be six times higher, as reported in the literature using 13X zeolite adsorbent, the cost is likely to be reduced to as low as \$94 /T-CO₂, which is lower than all other methods at a cost ranging from \$115 to \$220 /T-CO₂.

6.2 Future work

The feasibility of CO₂ enrichment by temperature swing adsorption directly from the air has been identified and economic analyses on the proposed method was carried out and compared with other CO₂ air capture approaches. The relatively high unit cost mainly results from the low adsorption and desorption performance of the adsorbent. As reported in the literature, some amine-based solid adsorbents, such as triamine-functionalized pore-expanded mesoporous silica (TRI-PE-MCM-41) and hyperbranched aminosilica (HAS), have shown much better adsorption and desorption performance. Therefore, for the future work, it is highly recommended to develop new adsorbents and evaluate the performance for temperature swing adsorption from air, with improved adsorption and desorption capacities. Only in this way can we lower the cost of such a competitive alternative to provide CO₂ to greenhouses compared with the existing CO₂ supply.

What is more, only economic analyses have been carried out in the present study. Besides the economics, the environmental impacts are other essential factors that people are concerned with. In the future, it is recommended that a complete life cycle analysis including environmental impact assessment be conducted on the proposed technology.

References

1. Eisenberger, P.M., et al., *Global Warming and Carbon-Negative Technology: Prospects for a Lower-Cost Route to a Lower-Risk Atmosphere*. Energy & Environment, 2009. **20**(6): p. 973-984.
2. Goepfert, A., et al., *Air as the renewable carbon source of the future: an overview of CO₂ capture from the atmosphere*. Energy & Environmental Science, 2012. **5**(7): p. 7833-7853.
3. Hansen, J., Ruedy, R., Sato, M., *Global Temperature Trends: 2005 Summation*. Technical report, NASA Goddard Institute for Space Studies, 2006.
4. Thomas, C.D., et al., *Extinction risk from climate change*. Nature, 2004. **427**(6970): p. 145-148.
5. *Canada's Emission Trends*, in *Environment Canada*. 2013, Government of Canada.
6. Choi, S., M.L. Gray, and C.W. Jones, *Amine-Tethered Solid Adsorbents Coupling High Adsorption Capacity and Regenerability for CO₂ Capture From Ambient Air*. Chemsuschem, 2011. **4**(5): p. 628-635.
7. Wang, T., K.S. Lackner, and A. Wright, *Moisture Swing Sorbent for Carbon Dioxide Capture from Ambient Air*. Environmental Science & Technology, 2011. **45**(15): p. 6670-6675.
8. Lackner, K.S.G., P.; Ziock, H., *Carbon Dioxide Extraction from Air?*, in *Los Alamos National Laboratory*. 1999: Los Alamos, NM.
9. Dion, L.M., M. Lefsrud, and V. Orsat, *Review of CO₂ recovery methods from the exhaust gas of biomass heating systems for safe enrichment in greenhouses*. Biomass & Bioenergy, 2011. **35**(8): p. 3422-3432.
10. LM, M., *Review: CO₂ enrichment in greenhouses. Crop responses*. Sci Hortic, 1987. **33**: p. 1-25.
11. Chalabi, Z.S., et al., *Optimal control strategies for carbon dioxide enrichment in greenhouse tomato crops part 1: Using pure carbon dioxide*. Biosystems Engineering, 2002. **83**(1): p. 127-127.
12. Wittwer S, R.W., *Carbon dioxide enrichment of greenhouse atmospheres for food crop production*. Econ Botany, 1964. **18**(34).
13. Jaffrin, A., et al., *Landfill biogas for heating greenhouses and providing carbon dioxide supplement for plant growth*. Biosystems Engineering, 2003. **86**(1): p. 113-123.
14. Sanchez-Guerrero, M.C., et al., *Effects of EC-based irrigation scheduling and CO₂ enrichment on water use efficiency of a greenhouse cucumber crop*. Agricultural Water Management, 2009. **96**(3): p. 429-436.
15. Willits, D.H. and M.M. Peet, *Predicting Yield Responses to Different Greenhouse Co₂ Enrichment Schemes - Cucumbers and Tomatoes*. Agricultural and Forest Meteorology, 1989. **44**(3-4): p. 275-293.
16. Tisserat, B., S.F. Vaughn, and M.A. Berhow, *Ultrahigh CO₂ levels enhances cuphea growth and morphogenesis*. Industrial Crops and Products, 2008. **27**(1): p. 133-135.

17. Critten, D.L. and B.J. Bailey, *A review of greenhouse engineering developments during the 1990s*. Agricultural and Forest Meteorology, 2002. **112**(1): p. 1-22.
18. Tisserat, B. and S.F. Vaughn, *Essential oils enhanced by ultra-high carbon dioxide levels from Lamiaceae species grown in vitro and in vivo*. Plant Cell Reports, 2001. **20**(4): p. 361-368.
19. Wang, S.Y., J.A. Bunce, and J.L. Maas, *Elevated carbon dioxide increases contents of antioxidant compounds in field-grown strawberries*. Journal of Agricultural and Food Chemistry, 2003. **51**(15): p. 4315-4320.
20. Jones, C.W., *CO₂ Capture from Dilute Gases as a Component of Modern Global Carbon Management*. Annual Review of Chemical and Biomolecular Engineering, Vol 2, 2011. **2**: p. 31-52.
21. (2007), I., *Climate Change 2007: Mitigation of Climate Change*.
22. Lackner, K.S.G., P.; Ziock, H., *Carbon dioxide extraction from air: Is it an option?*, in *The 24th International Conference on Coal Utilization and Fuel Systems*. 1999: FL.
23. Lackner, K.S., et al., *The urgency of the development of CO₂ capture from ambient air*. Proceedings of the National Academy of Sciences of the United States of America, 2012. **109**(33): p. 13156-13162.
24. Ha-Duong M, K.D.W., *Carbon Storage: The economic efficiency of storing CO₂ in leaky reservoirs*. Clean Technol Environ Policy, 2003(5): p. 181-189.
25. Tepe, J.B. and B.F. Dodge, *Absorption of carbon dioxide by sodium hydroxide solutions in a packed column*. Transactions of the American Institute of Chemical Engineers, 1943. **39**: p. 0581-0582.
26. Spector, N.A. and B.F. Dodge, *Removal of Carbon Dioxide from Atmospheric Air*. Transactions of the American Institute of Chemical Engineers, 1946. **42**(5-6): p. 827-848.
27. Blum, H.A., L.F. Stutzman, and W.S. Dodds, *Gas Absorption - Absorption of Carbon Dioxide from Air by Sodium and Potassium Hydroxides*. Industrial and Engineering Chemistry, 1952. **44**(12): p. 2969-2974.
28. Zeman F. S., L.K.S., *Capturing carbon dioxide directly from the atmosphere*. World Res. Rev., 2004. **16**: p. 157-172.
29. Keith, D.W., M. Ha-Duong, and J.K. Stolaroff, *Climate strategy with CO₂ capture from the air*. Climatic Change, 2006. **74**(1-3): p. 17-45.
30. Baciocchi, R., G. Storti, and M. Mazzotti, *Process design and energy requirements for the capture of carbon dioxide from air*. Chemical Engineering and Processing, 2006. **45**(12): p. 1047-1058.
31. Stolaroff, J.K., D.W. Keith, and G.V. Lowry, *Carbon dioxide capture from atmospheric air using sodium hydroxide spray*. Environmental Science & Technology, 2008. **42**(8): p. 2728-2735.
32. Mahmoudkhani, M. and D.W. Keith, *Low-energy sodium hydroxide recovery for CO₂ capture from atmospheric air-Thermodynamic analysis*. International Journal of Greenhouse Gas Control, 2009. **3**(4): p. 376-384.
33. Veselovskaya, J.V., et al., *Direct CO₂ capture from ambient air using K₂CO₃/Al₂O₃ composite sorbent*.

- International Journal of Greenhouse Gas Control, 2013. **17**: p. 332-340.
34. Zeman, F., *Energy and material balance of CO₂ capture from ambient air*. Environmental Science & Technology, 2007. **41**(21): p. 7558-7563.
 35. Socolow, R., Desmond, M., Aines, R., Blackstock, J., *Direct air capture of CO₂ with chemicals. A technology Assessment for the APS Panel on Public Affairs*. 2011.
 36. Lackner, K.S., *Capture of carbon dioxide from ambient air*. European Physical Journal-Special Topics, 2009. **176**: p. 93-106.
 37. Nikulshina, V., C. Gebald, and A. Steinfeld, *CO₂ capture from atmospheric air via consecutive CaO-carbonation and CaCO₃-calcination cycles in a fluidized-bed solar reactor*. Chemical Engineering Journal, 2009. **146**(2): p. 244-248.
 38. Nikulshina, V. and A. Steinfeld, *CO₂ capture from air via CaO-carbonation using a solar-driven fluidized bed reactor-Effect of temperature and water vapor concentration*. Chemical Engineering Journal, 2009. **155**(3): p. 867-873.
 39. Nikulshina, V., et al., *Feasibility of Na-based thermochemical cycles for the capture of CO₂ from air - Thermodynamic and thermogravimetric analyses*. Chemical Engineering Journal, 2008. **140**(1-3): p. 62-70.
 40. Lee, S.C., et al., *Development of new alumina-modified sorbents for CO₂ sorption and regeneration at temperatures below 200 degrees C*. Fuel, 2011. **90**(4): p. 1465-1470.
 41. Lee, S.C., et al., *CO₂ absorption and regeneration of alkali metal-based solid sorbents*. Catalysis Today, 2006. **111**(3-4): p. 385-390.
 42. Okunev, A.G., et al., *Sorption of carbon dioxide by the composite sorbent of potassium carbonate in porous matrix*. Russian Chemical Bulletin, 2003. **52**(2): p. 359-363.
 43. Sharonov, V.E., A.G. Okunev, and Y.I. Aristov, *Kinetics of carbon dioxide sorption by the composite material K₂CO₃ in Al₂O₃*. Reaction Kinetics and Catalysis Letters, 2004. **82**(2): p. 363-369.
 44. Tao Wang, J.L., Mengxiang Fang, Zhongyang Luo, *A Moisture Swing Sorbent for Direct Air Capture of Carbon Dioxide: Thermodynamic and Kinetic Analysis*. Energy Procedia, 2013. **37**: p. 6096-6104.
 45. Aaron, D. and C. Tsouris, *Separation of CO₂ from flue gas: A review*. Separation Science and Technology, 2005. **40**(1-3): p. 321-348.
 46. Serna-Guerrero, R., Y. Belmabkhout, and A. Sayari, *Triamine-grafted pore-expanded mesoporous silica for CO₂ capture: Effect of moisture and adsorbent regeneration strategies*. Adsorption-Journal of the International Adsorption Society, 2010. **16**(6): p. 567-575.
 47. Belmabkhout, Y. and A. Sayari, *Isothermal versus Non-isothermal Adsorption-Desorption Cycling of Triamine-Grafted Pore-Expanded MCM-41 Mesoporous Silica for CO₂ Capture from Flue Gas*. Energy & Fuels, 2010. **24**: p. 5273-5280.
 48. Li, G., et al., *Capture of CO₂ from high humidity flue gas by vacuum swing adsorption with zeolite 13X*.

- Adsorption-Journal of the International Adsorption Society, 2008. **14**(2-3): p. 415-422.
49. Ho, M.T., G.W. Allinson, and D.E. Wiley, *Reducing the cost of CO₂ capture from flue gases using pressure swing adsorption*. Industrial & Engineering Chemistry Research, 2008. **47**(14): p. 4883-4890.
 50. Lu, C.Y., et al., *Comparative study of CO₂ capture by carbon nanotubes, activated carbons, and zeolites*. Energy & Fuels, 2008. **22**(5): p. 3050-3056.
 51. Siriwardane, R.V., M.S. Shen, and E.P. Fisher, *Adsorption of CO₂ on zeolites at moderate temperatures*. Energy & Fuels, 2005. **19**(3): p. 1153-1159.
 52. Erten, Y., et al., *CO₂ adsorption and dehydration behavior of LiNaX, KNaX, CaNaX and CeNaX zeolites*. Journal of Thermal Analysis and Calorimetry, 2008. **94**(3): p. 715-718.
 53. Himeno, S., T. Komatsu, and S. Fujita, *Development of a new effective biogas adsorption storage technology*. Adsorption-Journal of the International Adsorption Society, 2005. **11**: p. 899-904.
 54. Zhou, L., et al., *Prediction of multicomponent adsorption equilibrium of gas mixtures including supercritical components*. Chemical Engineering Science, 2005. **60**(11): p. 2833-2844.
 55. Babarao, R., M. Eddaoudi, and J.W. Jiang, *Highly Porous Ionic rht Metal-Organic Framework for H₂ and CO₂ Storage and Separation: A Molecular Simulation Study*. Langmuir, 2010. **26**(13): p. 11196-11203.
 56. Cheng, Y., et al., *Reversible Structural Change of Cu-MOF on Exposure to Water and Its CO₂ Adsorptivity*. Langmuir, 2009. **25**(8): p. 4510-4513.
 57. Farha, O.K., et al., *Separating solids: Purification of metal-organic framework materials*. Journal of the American Chemical Society, 2008. **130**(27): p. 8598-8599.
 58. Li, W., et al., *Steam-Stripping for Regeneration of Supported Amine-Based CO₂ Adsorbents*. Chemsuschem, 2010. **3**(8): p. 899-903.
 59. Xu, X.C., et al., *Novel polyethylenimine-modified mesoporous molecular sieve of MCM-41 type as high-capacity adsorbent for CO₂ capture*. Energy & Fuels, 2002. **16**(6): p. 1463-1469.
 60. Xu, X.C., et al., *Preparation and characterization of novel CO₂ "molecular basket" adsorbents based on polymer-modified mesoporous molecular sieve MCM-41*. Microporous and Mesoporous Materials, 2003. **62**(1-2): p. 29-45.
 61. Xu, X.C., et al., *Influence of moisture on CO₂ separation from gas mixture by a nanoporous adsorbent based on polyethylenimine-modified molecular sieve MCM-41*. Industrial & Engineering Chemistry Research, 2005. **44**(21): p. 8113-8119.
 62. Tsuda, T. and T. Fujiwara, *Polyethyleneimine and Macrocyclic Polyamine Silica-Gels Acting as Carbon-Dioxide Absorbents*. Journal of the Chemical Society-Chemical Communications, 1992(22): p. 1659-1661.
 63. Tsuda, T., et al., *Amino Silica-Gels Acting as a Carbon-Dioxide Absorbent*. Chemistry Letters, 1992(11): p. 2161-2164.

64. Belmabkhout, Y., G. De Weireld, and A. Sayari, *Amine-Bearing Mesoporous Silica for CO₂ and H₂S Removal from Natural Gas and Biogas*. *Langmuir*, 2009. **25**(23): p. 13275-13278.
65. Belmabkhout, Y. and A. Sayari, *Adsorption of CO₂ from dry gases on MCM-41 silica at ambient temperature and high pressure. 2: Adsorption of CO₂/N₂, CO₂/CH₄ and CO₂/H₂ binary mixtures*. *Chemical Engineering Science*, 2009. **64**(17): p. 3729-3735.
66. Belmabkhout, Y. and A. Sayari, *Effect of pore expansion and amine functionalization of mesoporous silica on CO₂ adsorption over a wide range of conditions*. *Adsorption-Journal of the International Adsorption Society*, 2009. **15**(3): p. 318-328.
67. Belmabkhout, Y., R. Serna-Guerrero, and A. Sayari, *Amine-bearing mesoporous silica for CO₂ removal from dry and humid air*. *Chemical Engineering Science*, 2010. **65**(11): p. 3695-3698.
68. Harlick, P.J.E. and A. Sayari, *Applications of pore-expanded mesoporous silicas. 3. Triamine silane grafting for enhanced CO₂ adsorption*. *Industrial & Engineering Chemistry Research*, 2006. **45**(9): p. 3248-3255.
69. Harlick, P.J.E. and A. Sayari, *Applications of pore-expanded mesoporous silica. 5. Triamine grafted material with exceptional CO₂ dynamic and equilibrium adsorption performance*. *Industrial & Engineering Chemistry Research*, 2007. **46**(2): p. 446-458.
70. Franchi, R.S., P.J.E. Harlick, and A. Sayari, *Applications of pore-expanded mesoporous silica. 2. Development of a high-capacity, water-tolerant adsorbent for CO₂*. *Industrial & Engineering Chemistry Research*, 2005. **44**(21): p. 8007-8013.
71. Hicks, J.C., et al., *Designing adsorbents for CO₂ capture from flue gas-hyperbranched aminosilicas capable of capturing CO₂ reversibly*. *Journal of the American Chemical Society*, 2008. **130**(10): p. 2902-2903.
72. Goeppert, A., et al., *Carbon Dioxide Capture from the Air Using a Polyamine Based Regenerable Solid Adsorbent*. *Journal of the American Chemical Society*, 2011. **133**(50): p. 20164-20167.
73. Choi, S., et al., *Application of Amine-Tethered Solid Sorbents for Direct CO₂ Capture from the Ambient Air*. *Environmental Science & Technology*, 2011. **45**(6): p. 2420-2427.
74. Jain, *Pre-purification of air for separation*. 1993.
75. Sircar, S., Kratz, W.C., *Removal of water and carbon dioxide from air*. 1981.
76. Kumar, R., *Removal of water and carbon dioxide from atmosphere air*. 1987.
77. Rege, S.U., R.T. Yang, and M.A. Buzanowski, *Sorbents for air prepurification in air separation*. *Chemical Engineering Science*, 2000. **55**(21): p. 4827-4838.
78. Konduru, N., P. Lindner, and N.M. Assaf-Anad, *Curbing the greenhouse effect by carbon dioxide adsorption with zeolite 13X*. *Aiche Journal*, 2007. **53**(12): p. 3137-3143.
79. Merel, J., M. Clausse, and F. Meunier, *Carbon dioxide capture by indirect thermal swing adsorption using 13X zeolite*. *Environmental Progress*, 2006. **25**(4): p. 327-333.

80. Zhao, Z.L., et al., *Adsorption of carbon dioxide on alkali-modified zeolite 13X adsorbents*. International Journal of Greenhouse Gas Control, 2007. **1**(3): p. 355-359.
81. Su, F.S. and C.Y. Lu, *CO₂ capture from gas stream by zeolite 13X using a dual-column temperature/vacuum swing adsorption*. Energy & Environmental Science, 2012. **5**(10): p. 9021-9027.
82. Harlick, P.J.E. and F.H. Tezel, *An experimental adsorbent screening study for CO₂ removal from N₂*. Microporous and Mesoporous Materials, 2004. **76**(1-3): p. 71-79.
83. Wang, Z.M., T. Arai, and M. Kumagai, *Adsorption separation of low concentrations of CO₂ and NO₂ by synthetic zeolites*. Energy & Fuels, 1998. **12**(6): p. 1055-1060.
84. Kamiuto, K., S. Abe, and Ermalina, *Effect of desorption temperature on CO₂ adsorption equilibria of the honeycomb zeolite beds*. Applied Energy, 2002. **72**(3-4): p. 555-564.
85. Gael D. Ulrich, P.T.V., *Chemical Engineering Process Design and Economics*. 2 ed. 2004.
86. Hein, A.G., *Report on Greenhouse Energy Study*. 2000, Stothert Engineering Ltd.
87. Zhang, S., *Life Cycle Analysis of An Integrated Biogas-Based Agriculture Energy System*, in *Department of Chemical and Biological Engineering*. 2013, University of British Columbia.
88. Nikulshina, V., et al., *CO₂ capture from air and co-production of H₂ via the Ca(OH)₂-CaCO₃ cycle using concentrated solar power - Thermodynamic analysis*. Energy, 2006. **31**(12): p. 1715-1725.
89. Stolaroff, J.K., *Capturing CO₂ from ambient air: a feasibility assessment*. 2006, Carnegie Mellon University.